Nonsilica Oxide Glass Fiber Laser Sources: Part II

Chapter 7

Nonsilica Oxide Glass Fiber Laser Sources: Part II

Xiushan Zhu, Arturo Chavez-Pirson, Daniel Milanese, Joris Lousteau, Nadia Giovanna Boetti, Diego Pugliese and Nasser Peyghambarian

Additional information is available at the end of the chapter

http://dx.doi.org/10.5772/intechopen.74664

Abstract

Nonsilica oxide glasses have been developed and studied for many years as promising alternatives to the most used silica glass for the development of optical fiber lasers with unique characteristics. Their main properties and compositions, alongside the optical fiber fabrication principle, have been previously reviewed in part I. This chapter will review the development of optical fiber lasers operating in the infrared wavelength region based on nonsilica glass fiber materials, either phosphate, germanate or tellurite.

Keywords: nonsilica oxide glass, phosphate glass, germanate glass, tellurite glass, fiber laser, single-frequency fiber laser, mode-locked laser, high energy pulsed fiber laser, nonlinear wavelength conversion, supercontinuum

1. Introduction

The possibility to dope inorganic glasses with rare-earth (RE) ions has allowed the development of glass-based solid state lasers with various configurations, including bulk, microchip and optical fibers [1]. Optical fiber lasers and amplifiers, in particular, found applications in several fields, ranging from telecom (erbium-doped fiber amplifier, EDFA) to remote sensing (light detection and ranging, LIDAR), materials processing (high power lasers for marking, engraving and cutting) and medicine (for diagnosis and therapy of several diseases) [2].

The development of high power fiber lasers, up to 100 kW, did exploit the subsequent advances in engineering and manufacturing high purity silica optical preforms and fibers

originally intended for telecommunication applications [3]. The recent development of a fiber-based supercontinuum (SC) laser source with super high spectral power density was also made possible thanks to the low optical attenuation level achievable in silica glass and new photonic crystal fiber fabrication technology [4].

Despite its success, however, silica glass possesses several intrinsic limits, as detailed in part I, namely: a high phonon energy around 1100 cm^{-1} [5]; a limited rare-earth doping concentration level [6] and a short infrared transmission edge, which restricts its use for numerous high impact applications, such as mid-infrared (mid-IR) lasers, chemical sensing and infrared imaging [7].

The so-called soft glasses are based on alternative glass formers exhibiting different nature and structure, which offer alternative phonon energies and transmission characteristics, high rare-earth ions doping levels (up to 10^{21} ions/cm^3) and high optical nonlinearity (orders of magnitude higher than that exhibited by silica glass). Soft glasses include oxide and nonoxide glasses.

In this chapter, oxide-based soft glass fiber laser sources are reviewed, and the important aspect of soft glass fiber integration with standard optical components is also discussed. Wavelengths above 1400 nm belong to the so-called eye-safe range, where the eye fluids absorb part of the radiation and additionally the cornea cannot effectively focus the beam into the retina: lasers operating in this interval can be used outdoors at higher power levels without compromising the eye safety issue, being the maximum permissible exposure (MPE) higher [8]. Section 2 reports the main examples of phosphate glass fiber lasers, which mainly focus on emission wavelengths ranging from 1 to 1.5 μm. They include the following types of optical fiber laser sources: continuous-wave (CW) lasers, single-frequency lasers, high repetition rate mode-locked lasers and high energy amplifiers. Germanate fiber lasers are reviewed in Section 3, with a focus on emission wavelengths near or above 2 μm, where the glass composition performs at its best. Finally, Section 4 concerns the main types of tellurite fiber lasers, namely rare-earth-doped lasers and nonlinear wavelength conversion lasers.

2. Phosphate glass fiber lasers

As discussed in part I, the most attractive properties of phosphate glass are high solubility of rare-earth ions and low clustering effects. Therefore, highly doped phosphate fibers can be fabricated with low concentration quenching effects and are capable of producing very large unit gain (> 5 dB/cm). In addition, phosphate glass has large phonon energy and thus energy levels have short lifetimes, which enable high energy transfer rates between co-doped ions and reduce detrimental photodarkening effect. Owing to the high gain per unit length, highly Nd^{3+}-, Yb^{3+}- and Er^{3+}-doped phosphate fibers have been extensively used to develop a lot of short-length (from a few cm to tens of cm) lasers and amplifiers, including continuous-wave fiber lasers, single-frequency fiber lasers, high repetition rate mode-locked fiber lasers and high energy pulsed fiber amplifiers.

2.1. Continuous-wave phosphate fiber lasers

Phosphate fiber lasers were first demonstrated with Nd^{3+}- and Er^{3+}-doped phosphate fibers at 1054 and 1366 nm, and 1535 nm, respectively, by Yamashita in 1989 [9]. However, the output

powers of these fiber lasers using 10-mm long single-mode fibers were less than 1 mW. Later, much higher output power was obtained by using Nd^{3+}-doped multimode phosphate glass fibers [10]. In 2011, a watt-level single-mode Nd^{3+}-doped phosphate fiber laser was demonstrated with an output power of 2.87 W at 1053 nm and an efficiency of 44.7% [11]. However, due to the complicated structure of the energy levels, Nd^{3+}-doped fiber lasers are always susceptible to different detrimental effects, such as cross-relaxation, up-conversion, excited state absorption, etc., which constrain their power scaling. Compared to Nd^{3+}-doped fiber lasers, Yb^{3+}-doped fiber lasers are immune from these efficiency-reducing effects due to their simple energy level structure and are characterized by a lower quantum defect. The first 10-W level phosphate glass fiber laser at the 1 μm band was demonstrated with a 12 wt% Yb^{3+}-doped double-cladding phosphate fiber fabricated by NP Photonics [12]. Nearly 20 W output at 1.07 μm with a slope efficiency of 26.5% was obtained with an 86.4-cm long gain fiber pumped at 940 nm. When a 71.6-cm long 26 wt% Yb^{3+}-doped phosphate fiber was pumped at 977.6 nm, 57 W output at 1.06 μm with an efficiency of 50.6% was obtained even with a propagation loss of this fiber as high as 3 dB/m [13]. The output power of CW Yb^{3+}-doped phosphate fiber lasers is only constrained by the thermal issues. A 100-W level CW Yb^{3+}-doped phosphate fiber laser can be achieved by reducing the fiber loss and improving the fiber thermal management.

Compared to highly Nd^{3+}- and Yb^{3+}-doped phosphate fibers that have been generally used for short-length lasers at 1 μm, Er^{3+}-doped phosphate fibers are more attractive because they can provide very high gain per unit length at the 1.5 μm telecommunication window and thus very short length Er^{3+}-doped fiber amplifiers (EDFAs) can be developed for optical communications. A highly Er^{3+}-doped phosphate fiber was first used for laser amplification at NP Photonics in 2001 [14]. A net gain of 21 dB and a gain per unit length of 3 dB/cm were achieved in a 71-mm long 3.5 wt% Er^{3+}-doped phosphate fiber. Super compact gain module very suitable for signal amplification for local area networks (LANs) has been developed with highly Er^{3+}-doped phosphate fiber as shown in **Figure 1(a)**. The length of the pencil-like gain block is less than 10 cm and its diameter is 3–6 mm. Over 22 dB peak gain and over 15 nm of 10 dB bandwidth have been obtained with such a compact gain module as shown in **Figure 1(b)**. Over 40 dB peak gain can be obtained when a dual-end pumping configuration is used.

The gain or output power of a core-pumped Er^{3+}-doped phosphate fiber amplifier is usually limited by the maximum available power of single-mode pump lasers. In order to increase the gain or output power, double-cladding Er^{3+}/Yb^{3+} co-doped phosphate fibers have been fabricated for cladding-pumping with multimode pump diodes. Due to the high rare-earth solubility and large phonon energy typical of the phosphate glass, highly Er^{3+}/Yb^{3+} co-doped phosphate fibers have very high cladding absorption at 980 nm and very efficient energy transfer from Yb^{3+} to Er^{3+}.

In 2015, high concentration Er^{3+}/Yb^{3+} co-doped double-cladding phosphate fibers have been reported with high gain per unit length, specifically 2.3 dB/cm in cladding-pumping configuration and 4.0 dB/cm in core-pumping arrangement [15].

Several watt-level Er^{3+}/Yb^{3+} co-doped phosphate fiber lasers at the 1.5 μm band have been demonstrated [16–18]. As shown in **Figure 2(a)**, more than 9 W CW 1535 nm multimode output was obtained with a 7.0 -cm long 20-μm core Er^{3+}/Yb^{3+} co-doped phosphate fiber, corresponding to a very high output power per unit fiber length of 1.33 W/cm. Diffraction-limited output with

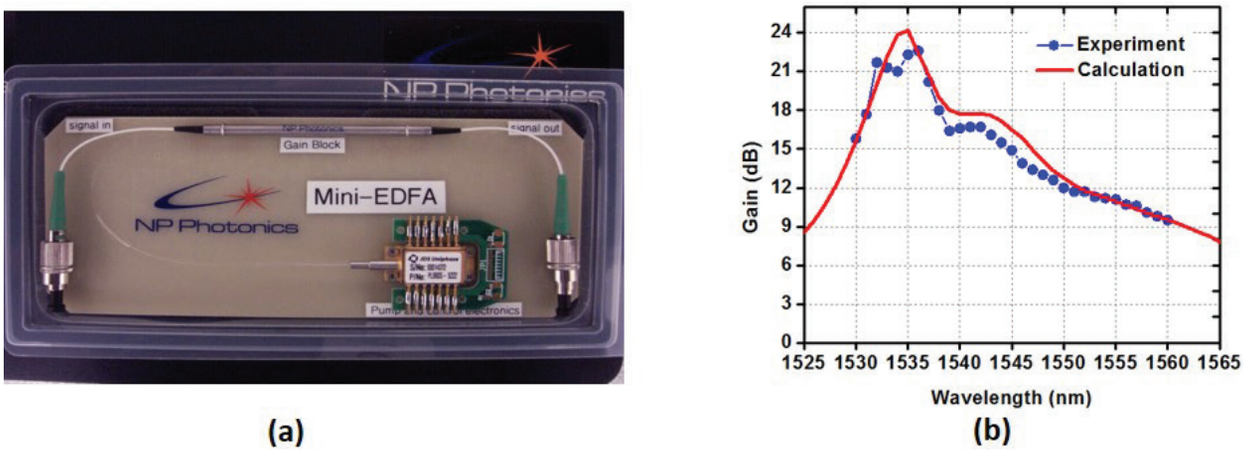

Figure 1. (a) Photograph of a NP photonics mini-EDFA with a pencil-like gain module pumped by a fiber-coupled laser diode; (b) calculated and measured gain of the NP photonics mini-EDFA.

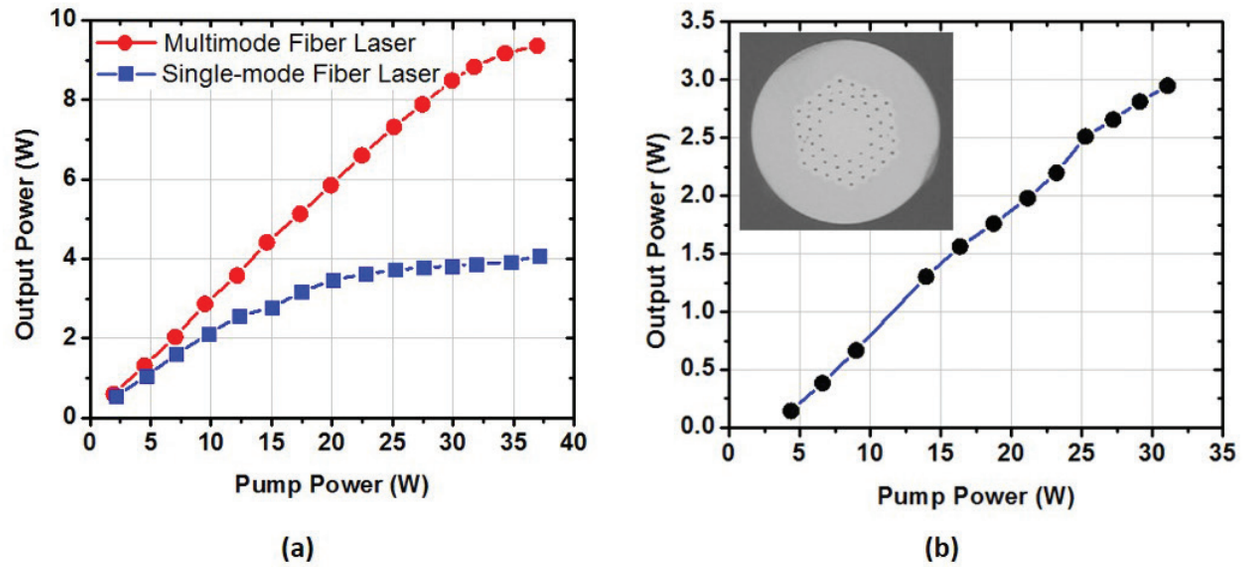

Figure 2. (a) Output power as a function of the pump power for a multimode and a single-mode Er^{3+}/Yb^{3+} co-doped phosphate fiber laser; (b) output power of an Er^{3+}/Yb^{3+} co-doped microstructured phosphate fiber laser as a function of the pump power. Inset: Microscope image of the microstructured phosphate fiber.

an output power of 4 W and $M^2 = 1.1$ was generated with a 7.1-cm long single-mode Er^{3+}-Yb^{3+} co-doped phosphate fiber with a core diameter of 13 μm and core numerical aperture (NA) of 0.08. Phosphate glass microstructured fiber with an active core area larger than 400 mm^2 was also fabricated as shown in **Figure 2(b)** and more than 3 W near diffraction-limited output was obtained with a 11-cm long Er^{3+}/Yb^{3+} co-doped phosphate microstructured fiber.

Although the CW output powers of the highly doped phosphate fiber lasers presented here are much lower than those of the counterpart silica fiber lasers, these experiments have shown the potential and promise of producing high energy single-frequency lasers and ultrashort lasers by using short-length highly doped phosphate fibers, in which the accumulated nonlinearity is significantly reduced.

2.2. Single-frequency phosphate fiber lasers

Single-frequency lasers operating with only a single-longitudinal mode can emit quasi-monochromatic radiation with very narrow linewidth and ultralow noise. Conventional fiber lasers generally consist of meters of fiber with linear cavity configuration and thus cannot generate single-frequency laser output due to the spatial hole burning. Unidirectional ring cavity combined with a narrow-band filter and a very short linear cavity combined with narrow-band fiber Bragg gratings (FBGs) are two major approaches to achieve single-frequency fiber lasers. However, ring cavity single-frequency fiber lasers usually suffer from second mode and mode hopping. Both distributed Bragg reflector (DBR) and distributed feedback (DFB) fiber lasers with a several centimeter long cavity can offer robust single-frequency operation without mode hopping. But the output power of a DFB single-frequency fiber laser is limited due to the very short length of the gain fiber. Moreover, the stability of DFB fiber lasers is low because the FBG is inscribed in the gain fiber where thermal noises will greatly impair the performance of the laser. DBR single-frequency fiber laser can provide robust single-frequency operation at watt-level output power and at sub-kilohertz linewidth. DBR single-frequency fiber lasers also offer easy and convenient way to tune and stabilize the laser wavelength due to their unique configuration. As depicted in **Figure 3(a)**, a DBR single-frequency fiber laser consists of a short piece of gain fiber and two fiber Bragg gratings (FBGs). The free spectral range of a laser cavity is defined as:

$$\Delta\nu = \frac{c}{2nL} \tag{1}$$

where c is the light speed, n is the refractive index of the optical fiber core and L is the length of the fiber laser cavity. Therefore, robust single-frequency operation of a fiber laser can be obtained only when L is very short and the free spectral range of the laser cavity is so large that only one longitudinal mode is allowed to oscillate within the narrow bandwidth of the

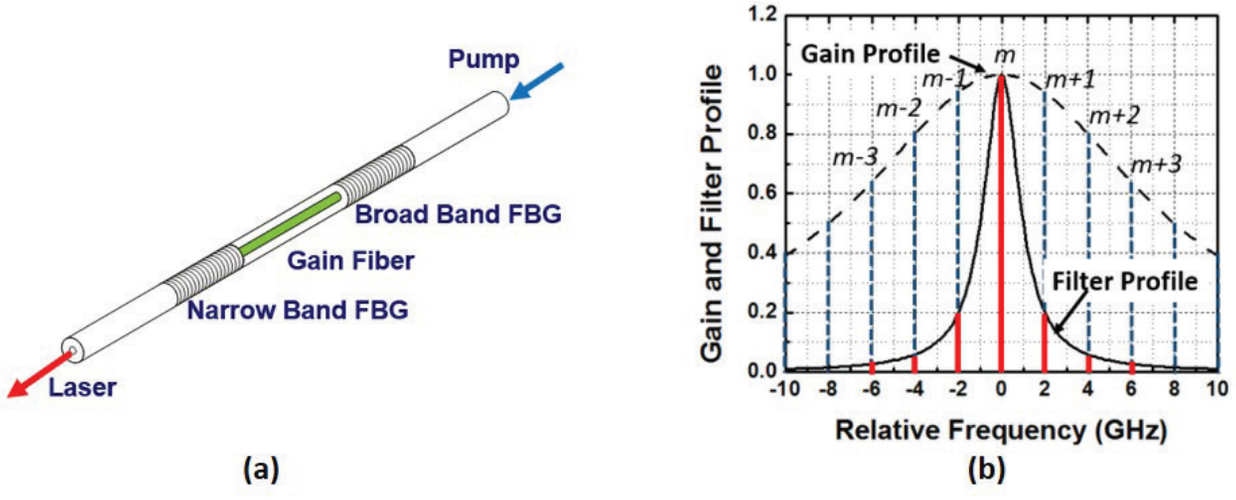

Figure 3. (a) The configuration of a DBR single-frequency fiber laser; (b) single-longitudinal mode operation of a short-length DBR laser ensured by the narrow bandwidth transmission of a FBG.

narrow-band FBG, as depicted in **Figure 3(b)**. Highly doped phosphate glass fibers exhibiting extremely high optical gain per unit length with negligible ion clustering are uniquely suitable for short-length linear cavity single-frequency fiber lasers.

A highly Er^{3+}/Yb^{3+} co-doped phosphate fiber was first used to develop a DBR single-frequency fiber laser at 1560 nm with an output power higher than 200 mW and a very narrow linewidth of less than 2 kHz [19]. Single-frequency fiber lasers exhibit excellent features of low noises, high stability and narrow spectral linewidth, which are usually characterized by optical signal-to-noise ratio (SNR), relative intensity noise (RIN), frequency noise and spectral linewidth. The optical SNR of a single-frequency fiber laser is usually measured with an optical spectrum analyzer using the highest spectral resolution. A typical spectrum of a 1550 nm single-frequency fiber laser is shown in **Figure 4(a)**, exhibiting over 85 dB optical SNR. The RIN is a key parameter to characterize the optical power fluctuation of a laser. The typical RIN of a single-frequency fiber laser is shown in **Figure 4(b)**. The RIN typically has a peak at the relaxation oscillation frequency of the laser and then decreases with the increased frequency until it converges to the shot noise level. The relaxation frequency peak of the RIN can usually be suppressed with a close-loop servo system as shown in the inset of **Figure 4(b)**. The frequency noise is the random fluctuation of the instantaneous frequency of a single-frequency laser. The frequency noise is generally directly measured by frequency discriminators, which convert frequency fluctuation to intensity fluctuation and then measure the power spectral density. The measured frequency noise of DBR single-frequency fiber lasers at 1550 and 1060 nm is shown in **Figure 4(c)**. The frequency noise typically decreases with the increased frequency and exhibits some spikes related to various noises. Due to the various laser noises, a single-frequency laser is not perfectly monochromatic and has finite spectral linewidths. The spectral linewidth of a single-frequency fiber laser is usually measured with heterodyne detection and delayed self-heterodyne detection methods. A linewidth measurement result of a noise-suppressed DBR single-frequency fiber laser at 1550 nm assessed with the delayed self-heterodyne detection method is shown in **Figure 4(d)**. A very narrow spectral linewidth of 500 Hz can be estimated from the −20 dB spectral bandwidth of 10.5 kHz.

The output power of a core-pumped single-frequency fiber laser is limited by the available pump power of single-mode pump diodes and is generally at a level of few hundreds of mW. A higher output power of a single-frequency fiber laser can be achieved with cladding-pumping. A cladding-pumped monolithic all-phosphate glass single-frequency fiber laser was demonstrated by inscribing FBGs directly into heavily Er^{3+}/Yb^{3+} co-doped phosphate glass fiber using femtosecond laser pulses and a phase mask [20]. A robust single-frequency output with power up to 550 mW and a spectral linewidth less than 60 kHz was obtained. In Ref. [21], a 1.6 W single-frequency fiber laser was demonstrated with a double-cladding phosphate fiber with a 18 μm core doped with 1 wt% Er^{3+} and 8 wt% Yb^{3+} ions and a 125 μm cladding.

In addition to single-frequency fiber lasers operating at the 1.5 μm band, several single-frequency fiber lasers at the 1 μm band developed with highly Yb^{3+}-doped phosphate fibers were reported [22–25]. Over 400 mW single-frequency laser output at 1.06 μm was achieved from a 0.8-cm long 15.2 wt% Yb^{3+}-doped phosphate fiber [22]. The measured slope efficiency and estimated quantum efficiency of laser emission are 72.7% and 93%, respectively. In Ref. [23], an all-fiber actively Q-switched single-frequency fiber laser at 1064 nm was developed by using a piezoelectric to

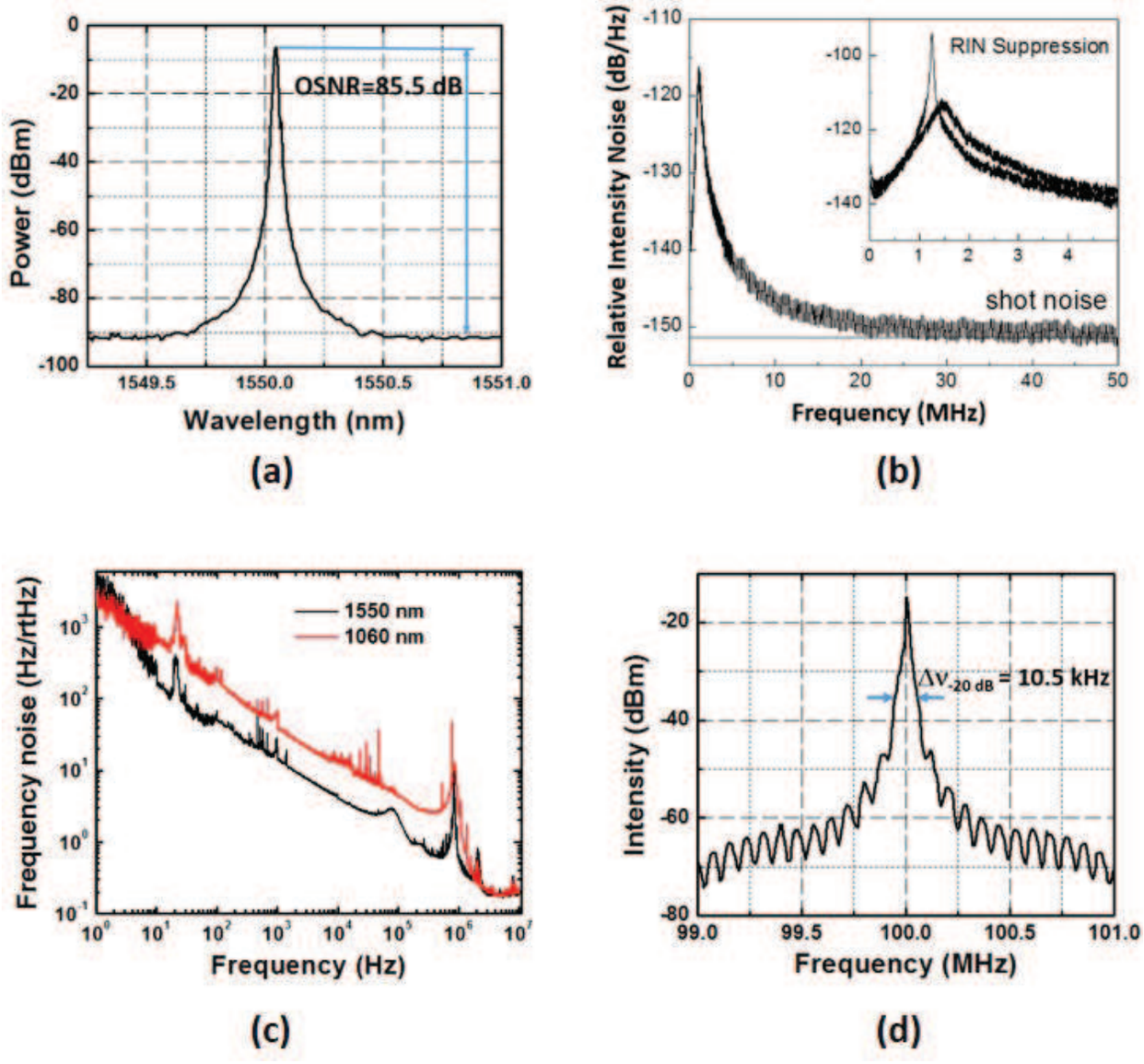

Figure 4. (a) Optical spectrum and (b) RIN of a DBR single-frequency fiber laser at 1550 nm; (c) frequency noises of DBR single-frequency fiber lasers at 1060 and 1550 nm; (d) typical spectral linewidth measurement result of self-delayed heterodyne detection for a DBR single-frequency fiber laser at 1550 nm.

press the fiber and modulate the fiber birefringence. Q-switched single-frequency laser operation at repetition rates tunable from several Hz to up to 700 kHz was demonstrated. In 2016, a single-frequency Yb^{3+} fiber laser operating at a wavelength longer than 1100 nm was demonstrated with a 3.1-cm long 15.2 wt% Yb^{3+}-doped phosphate fiber [24]. More than 62 mW single-frequency laser output with a linewidth of 5.7 kHz was obtained.

Highly Yb^{3+}-doped phosphate fibers have also been used to develop single-frequency laser sources at 976 nm, which are highly demanded for nonlinear wavelength conversion to generate coherent blue light at the 488 nm argon-ion laser wavelength. The energy level diagram of Yb^{3+} ions is shown in **Figure 5(a)**. The ground state absorption of the 915 nm pump corresponds to a transition from the lowest level of the $^2F_{7/2}$ manifold to the upper level of the $^2F_{5/2}$ manifold. The transition from the lowest level of the excited state $^2F_{5/2}$ manifold to the lowest level of the

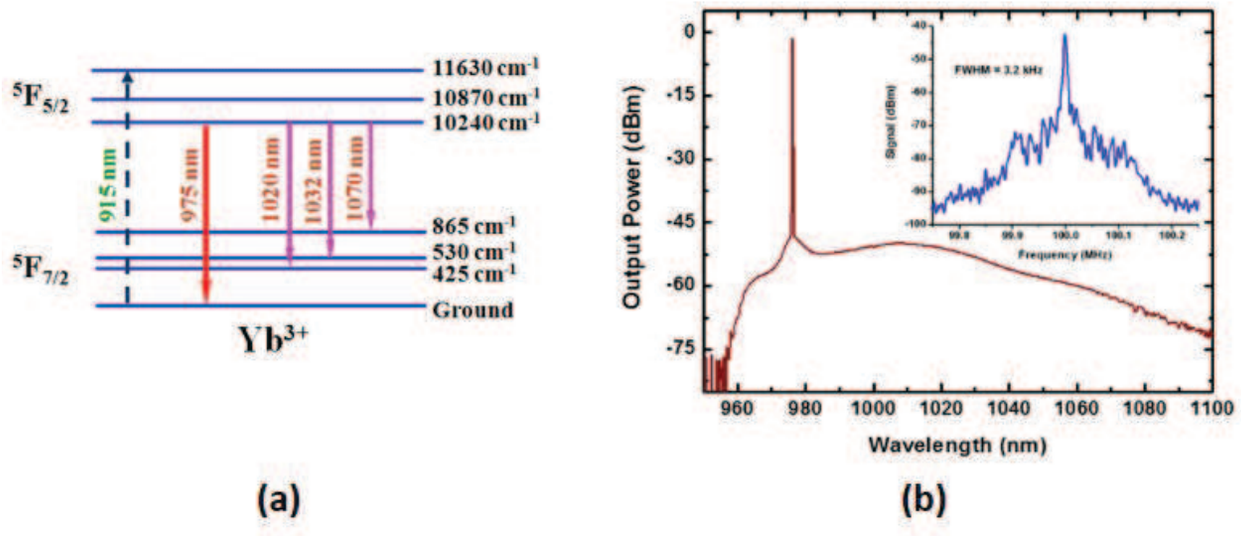

Figure 5. (a) The energy level diagram of Yb^{3+} ions; (b) optical spectrum of a 976 nm single-frequency fiber laser. Inset: Spectral linewidth measurement result of self-delayed heterodyne detection for the 976 nm single-frequency fiber laser.

ground state $^2F_{7/2}$ manifold produces the laser emission at 976 nm. A DBR single-frequency fiber laser at 976 nm was first developed with a 2-cm long 6 wt% Yb^{3+}-doped phosphate fiber and a pair of silica FBGs [25]. More than 100 mW of linearly polarized output were achieved from the all-fiber DBR laser with a linewidth less than 3 kHz. **Figure 5(b)** shows the optical spectrum and the spectral linewidth measurement result of the 976 nm single-frequency fiber laser.

In order to further increase the power level of the 976 nm single-frequency fiber lasers, core- and cladding-pumped highly Yb^{3+}-doped phosphate fiber amplifiers have been investigated [25, 26]. A 6 wt% Yb^{3+}-doped phosphate polarization maintaining (PM) fiber with a core diameter of 6 μm and a core NA of 0.14 as shown in the inset of **Figure 6(a)** was used for the investigations of core-pumped single-frequency fiber amplifiers [25]. **Figure 6(a)** shows the experimental results, and over 350 mW linearly polarized output with a slope efficiency of 52.5% was obtained from a 4-cm long fiber amplifier. A small signal net gain of 25 dB, corresponding to a unit gain of over 6 dB/cm, was achieved with this fiber. The output power of the core-pumped fiber amplifier is limited by the available single-mode pump power at 915 nm. In order to further increase the 976 nm single-frequency laser output, cladding-pumping with multimode diodes has to be used. The inset of **Figure 6(b)** shows the microscopic image of an Yb^{3+}-doped double-cladding phosphate fiber that was used to investigate the power scaling of a 976 nm single-frequency fiber amplifier. This double-cladding phosphate fiber, characterized by a core diameter of 18 μm and a core NA of 0.04, is able to support only the fundamental transverse mode at 976 nm. The inner circular cladding has a diameter of 135 μm and a NA of 0.45. The outer cladding is also made of phosphate glass and its diameter is 150 μm. The core was uniformly doped with 6 wt% Yb^{3+} ions. The output powers of the cladding-pumped fiber amplifiers with different gain fiber lengths (L_f) were measured as shown in **Figure 6(b)**. The output powers of the 6.5, 7, 8 and 10-cm long fiber amplifiers are 2.58, 3.41, 3.14 and 3.12 W, respectively, at the maximum launched pump power of 70 W. The slope efficiencies of the cladding-pumped fiber amplifiers are much lower than those of the core-pumped fiber amplifiers. This is mainly due to the relatively low spatial

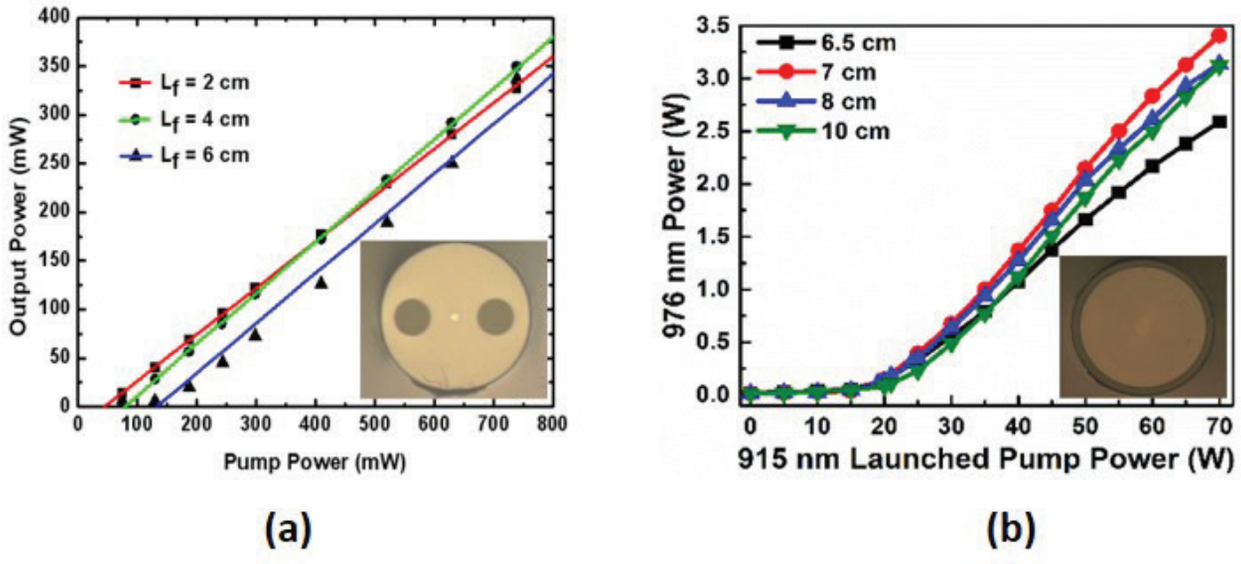

Figure 6. (a) Output power as a function of the pump power of core-pumped single-frequency Yb^{3+}-doped phosphate fiber amplifiers at 976 nm. Inset: Microscopic image of a 6 μm core PM 6 wt% Yb^{3+}-doped phosphate fiber. (b) Output power as a function of the pump power of cladding-pumped single-frequency Yb^{3+}-doped phosphate fiber amplifiers at 976 nm. Inset: Microscopic image of an 18 μm core 6 wt% Yb^{3+}-doped phosphate fiber.

overlap between the pump and the doped fiber core in the cladding-pumping configuration. The output power and the efficiency of the cladding-pumped single-frequency laser fiber amplifier can be significantly improved by using a phosphate fiber with an optimal concentration, a small inner cladding, a large core and a specific waveguide to suppress the long wavelength amplified spontaneous emission (ASE).

2.3. High repetition rate mode-locked phosphate fiber lasers

High repetition rate mode-locked lasers are essentially needed in many fields of science and industry, including material processing, accelerator applications, frequency comb spectroscopy, metrology and coherent control. Passively mode-locked fiber lasers have shown their capability of generating transform-limited pulses in the picosecond regime due to their simplicity and reliability. A drawback of the conventional passively mode-locked fiber lasers is that the pulse repetition rate is at a level of tens of MHz due to the long cavity length (several meters). The repetition rate f_{rep} of a linear cavity fiber laser operating in the fundamental mode locking is expressed as:

$$f_{rep} = \frac{c}{2nL} \tag{2}$$

where L is the cavity length, n is the effective refractive index and c is the velocity of the light in vacuum. To obtain a GHz repetition rate mode-locked fiber laser, the fiber length has to be less than 10 cm. Due to the low absorption coefficient of a conventional silica fiber, which is limited by the low RE solubility of silica glass, it is hard to generate a high-efficiency GHz repetition rate mode-locked laser using conventional silica fiber laser technology. This problem can be solved with highly doped phosphate fiber laser technology.

Because of the extremely high absorption of the highly doped phosphate fibers, mode-locked laser oscillators in all-fiber format with excellent stability and reliability can be developed. As shown in **Figure 7(a)**, an all-fiber mode-locked laser at 1034 nm was made by splicing a 5-cm long 6 wt% Yb^{3+}-doped phosphate fiber to a 3-cm long chirped FBG and the 2-cm long pigtail of a fiber-optic semiconductor saturable absorber mirror (SESAM). The total length of the mode-locked fiber laser cavity is about 10 cm, corresponding to a repetition rate of 1 GHz. The pulse train of this laser was measured by a fast photodetector and is shown in **Figure 7(b)**. The optical spectrum of the 1 GHz repetition rate mode-locked fiber laser is shown in **Figure 7(c)**. The pulse width of this laser was measured by an auto-correlator to be about 16 ps.

The total length of a chirped FBG usually needs to be 3 cm or more so that its bandwidth is sufficiently broad to support the operation of a mode-locked laser. Therefore, a chirped FBG cannot be used to develop an all-fiber mode-locked fiber laser as its repetition rate is larger than 3 GHz. A fiber mirror fabricated by depositing a dichroic thin film onto the fiber end-face can be used as the cavity coupler of a fiber laser. Therefore, the fiber cavity length can be 1 cm or shorter and 10 GHz repetition rate mode-locked fiber lasers can be developed. The first 10 GHz repetition rate mode-locked fiber laser was reported in 2007 [27]. A heavily Er^{3+}/Yb^{3+} co-doped phosphate fiber was used to form 1-cm long cavity with fiber mirrors. Stable mode-locked pulse trains with output power as high as 30 mW at 1535 nm were obtained. In [28], a compact and stable all-fiber fundamentally mode-locked laser system with a repetition rate of 12 GHz was developed with the configuration shown in **Figure 8(a)**. The self-starting mode-locked laser consists of a SESAM with low modulation depth and a high gain per unit length and a polarization maintaining 0.8-cm long Er^{3+}/Yb^{3+} phosphate fiber as gain medium. The optical spectrum of the 12 GHz repetition rate mode-locked fiber laser is shown in **Figure 8(b)**. The 12 GHz repetition rate was confirmed by the modulation of the high resolution (0.01 nm) spectrum. This mode-locked fiber laser has a temporal pulse width of ~2.3 ps and an average power of 5 mW at a pump power of 400 mW. The timing jitter has been measured using an optical cross-correlation method and found to be 44 fs/pulse.

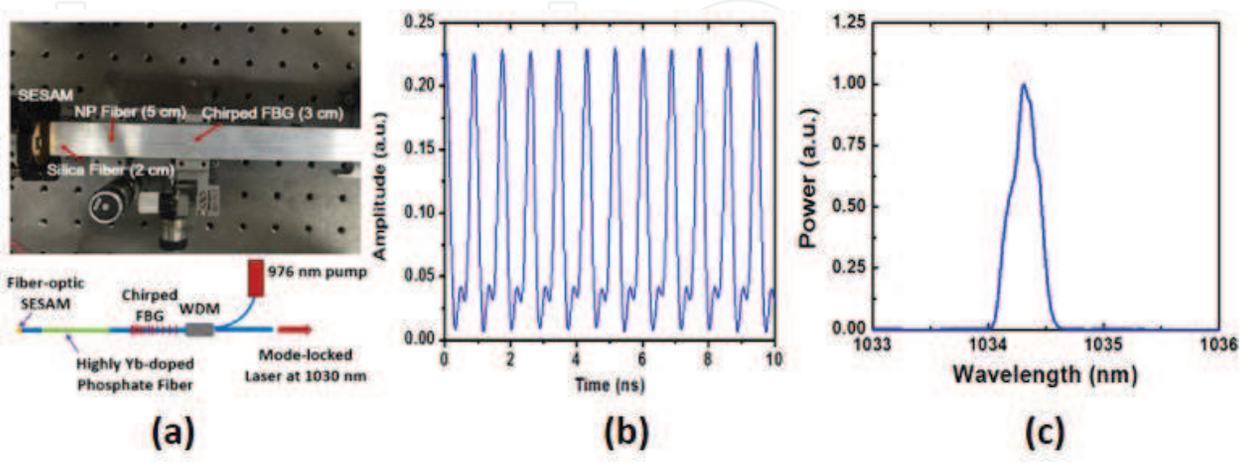

Figure 7. (a) Configuration and setup, (b) pulse train and (c) optical spectrum of a monolithic 1 GHz repetition rate mode-locked Yb^{3+}-doped phosphate laser.

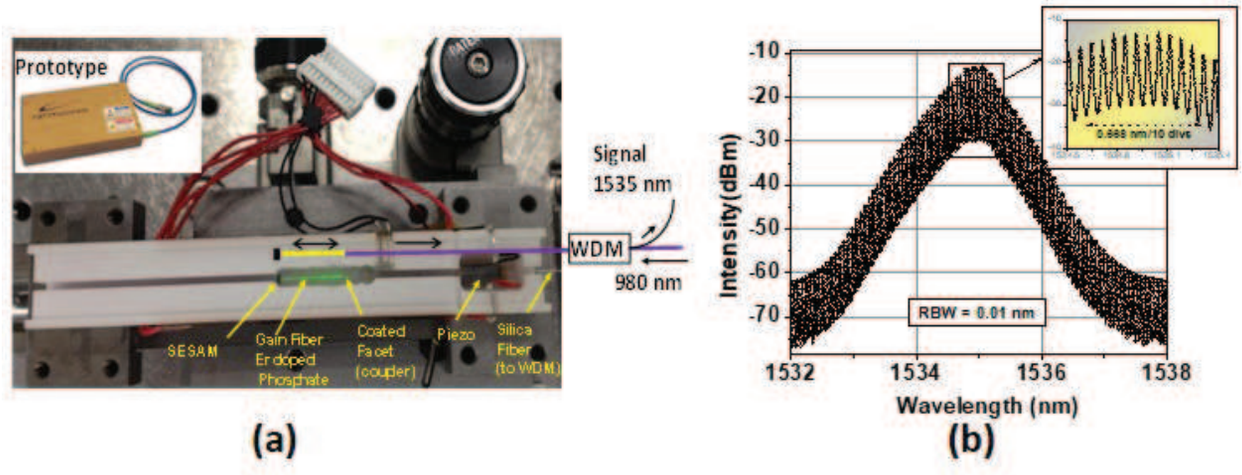

Figure 8. (a) The experimental setup and (b) output optical spectrum of a 12 GHz repetition rate SESAM mode-locked Er^{3+}-doped phosphate fiber laser.

2.4. High energy phosphate fiber amplifiers

The energy of a pulsed laser oscillator is generally much lower than the levels required for the applications. Fiber amplifiers have been extensively used to scale up the power/energy of a laser system because of their high single-pass gains and excellent heat dissipation capability. However, due to the inherent long interaction length of a conventional silica fiber amplifier, its output energy is usually constrained by nonlinear effects including self-phase modulation (SPM), stimulated Raman scattering (SRS), stimulated Brillouin scattering (SBS) and four-wave mixing (FWM), which deform the pulses both in temporal and spectral domains. Highly rare-earth doped phosphate fibers allow the construction of rather short fiber amplifiers enabling high energy pulse amplification less prone to nonlinear distortions. In addition, the nonlinear refractive index of phosphate glass is three times lower and the SBS gain cross-section is 50% weaker than those of silica glass. Moreover, the photodarkening effect in phosphate glass is also much less pronounced than in silica glass [29]. Therefore, highly doped phosphate glass fibers are excellent energy engines for a high energy fiber laser system.

High energy single-frequency laser sources are in great demand for a variety of applications including LIDAR, remote sensing, free-space communication and laboratory research. However, the power scaling of single-frequency lasers has been difficult to obtain in fiber amplifiers due to limitations primarily related to the SBS, which converts a fraction of the desired laser light to a backscattered Stokes-shifted reflection. SBS builds up strongly in the fiber because of the long interaction length and small mode field area. So, it has been difficult to achieve high peak power, single-transverse mode and narrow linewidth operation simultaneously in a fiber laser system, especially for a monolithic all-fiber configuration. The threshold for SBS in an optical fiber is determined by the parameters of the fiber to be:

$$P_{th} = \frac{21\,A_{eff}}{L_{eff}\,g_B} \tag{3}$$

where A_{eff} is the effective mode field area, L_{eff} is the effective length of the optical fiber and g_B is the SBS gain of the glass fiber. Therefore, using short length and large core fiber is a key approach to elevate the peak and average powers for single-frequency lasers. Highly doped phosphate fibers with large mode area have been widely used to achieve nanosecond single-frequency pulses at the 1 and 1.55 μm bands [30–34].

Figure 9(a) shows the output pulse energy and peak power of a highly Yb^{3+}-doped phosphate fiber amplifier for 1064 nm 2 ns pulsed single-frequency laser [33]. The 6 wt% Yb^{3+}-doped phosphate fiber has a core diameter of 25 μm and a cladding of 250 μm, as shown in the inset of **Figure 9(a)**. An average power of 32 W, a pulse energy of 90 μJ and a peak power of 45 kW were obtained with a 45-cm long gain fiber at a pump power of 55 W. **Figure 9(b)** shows the output pulse energy and peak power of a highly Er^{3+}/Yb^{3+} co-doped phosphate fiber amplifier for 1530 nm 105 ns pulsed single-frequency laser [34]. The fiber core is doped with 3 wt% Er^{3+} and 15 wt% Yb^{3+}. The core and cladding diameters of this fiber are 25 and 400 μm, respectively. A single-frequency pulsed laser with a peak power of 1.2 kW at a repetition rate of 8 kHz, corresponding to a pulse energy of 126 μJ, was obtained with a 15 -cm long gain fiber at a pump power of 75 W. When the pulse width of the single-frequency pulses is 10 ns, over 50 kW peak power has also been achieved with a SBS-free highly Er^{3+}/Yb^{3+} co-doped phosphate fiber amplifier [30, 32].

High energy ultrashort pulsed laser sources have enormous impact on many disciplines of science and technology. Solid state mode-locked laser sources, namely Ti:sapphire lasers, have shown their excellence in producing high energy ultrashort pulses. However, Ti:sapphire laser sources usually operate with repetition rates in the kilohertz range, and the output power is still at watt level limited by the thermal issues and low efficiencies. The fast acquisitions and high yields of various applications are currently boosting demands for ultrafast laser sources with high average power and high repetition rate. Fiber amplifiers are high-efficiency energy engine for power scaling of high repetition rate mode-locked lasers. However, the energy

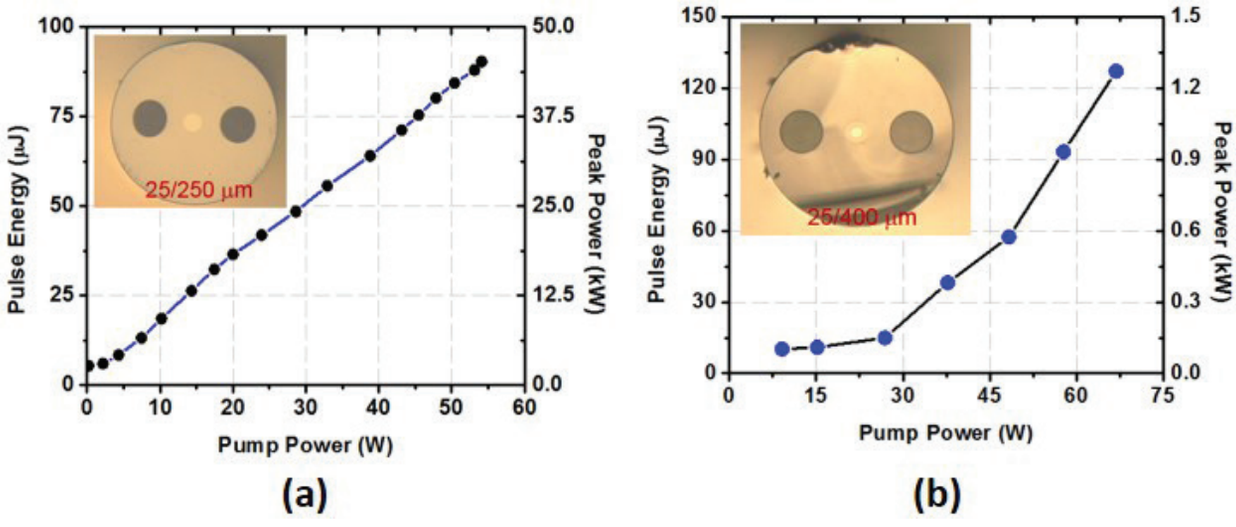

Figure 9. (a) Pulse energy and peak power of a 25/250 μm Yb^{3+}-doped phosphate fiber amplifier for 1064 nm 2 ns single-frequency laser; (b) pulse energy and peak power of a 25/400 μm Er^{3+}/Yb^{3+} co-doped phosphate fiber amplifier for 1530 nm 105 ns single-frequency laser.

scaling of a mode-locked fiber laser system usually suffers from pulse distortion caused by SPM as the pulses propagate through the fiber. The magnitude of the SPM is quantified by the *B*-integral and is proportional to both the beam irradiance inside the amplifier and the propagation length, as shown in the following equation:

$$B = \frac{2\pi}{\lambda}\int_0^L n_2 I(z)dz = \frac{2\pi}{\lambda A_{eff}}\int_0^L n_2 P(z)dz \quad (4)$$

where λ is the laser wavelength, n_2 is the nonlinear refractive index coefficient, $I(z)$ is the pulse peak irradiance along the propagation direction, $P(z)$ is the pulse peak power, L is the total fiber length and A_{eff} is the fiber effective mode area. A *B*-integral of less than π radians is considered linear propagation. Above this value, nonlinear phase accumulation will impose temporally broadened pulses and/or significant pulse pedestal. Therefore, compared to several meters of silica fiber amplifiers, sub-50 cm highly doped phosphate fiber amplifiers are more favorable for mode-locked laser amplification because much less nonlinear distortion is experienced. Highly doped phosphate fiber amplifiers have already been used to demonstrate direct picosecond pulse amplification with low distortion and achieve mJ-level femtosecond laser using the chirped pulse amplification technique [35–37].

Figure 10(a) shows the output average power of a 6 wt% Yb^{3+}-doped phosphate amplifier for direct amplification of 1.86 MHz repetition rate picosecond pulses at 1064 nm. The Yb^{3+}-doped phosphate fiber has a core size of 25 μm and a cladding size of 250 μm. Over 20 W output power was obtained with a 40-cm long gain fiber at a pump power of 40 W. In [35], a 1 wt% Er^{3+} and 8 wt% Yb^{3+} co-doped phosphate fiber amplifier was used to directly amplify picosecond mode-locked pulses at 1.55 μm. An average output power of 1.425 W at a repetition rate of 70 MHz, corresponding to a pulse energy and peak power of 20.4 nJ and 16.6 kW, respectively, was obtained with a 15 cm long fiber with a core size of 14 μm. In [36], a 2 wt% Er^{3+}-doped phosphate

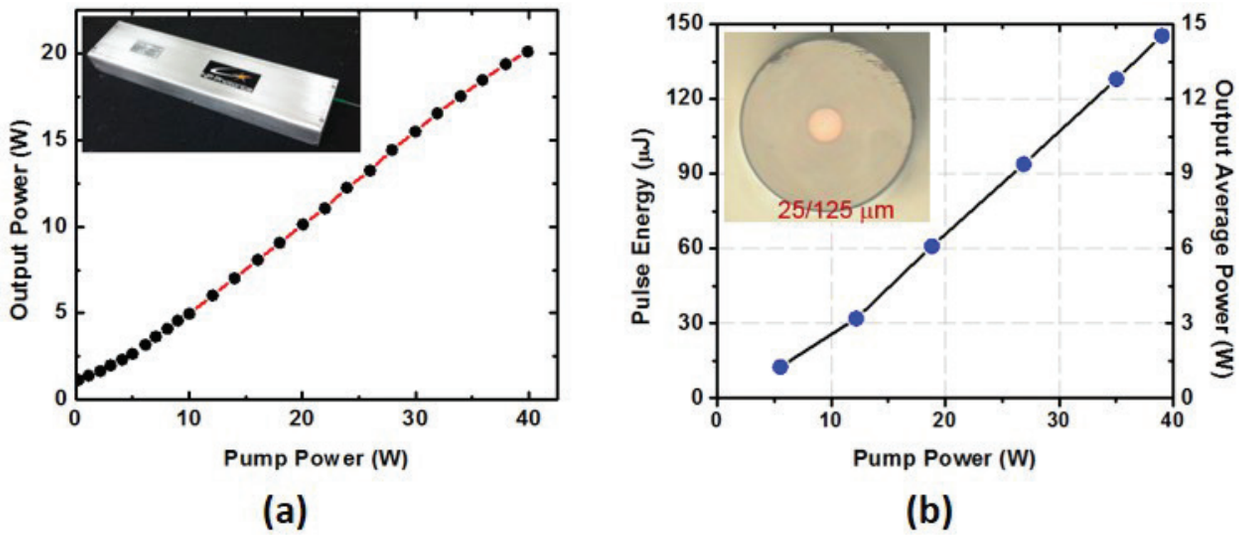

Figure 10. (a) Output average power of an Yb^{3+}-doped phosphate fiber amplifier module (shown in the inset) for 1064 nm 1 MHz 15 ps mode-locked laser; (b) pulse energy and average power of a 25/125 μm Er^{3+}-doped phosphate fiber amplifier for 100 kHz mode-locked laser at 1550 nm.

fiber with a core size of 25 μm and a cladding of 125 μm was fabricated as shown in the inset of **Figure 10(b)** for in-band high-efficiency chirped pulse amplification of a 1.55 μm mode-locked laser. As shown in **Figure 10(b)**, ultrashort pulses with pulse energy >140 μJ and average power of 14 W were obtained with a 20-cm long gain fiber at a 1480 nm pump power of 40 W. A peak power of ~160 MW was obtained with the compressed pulses. This 2 wt% Er^{3+}-doped phosphate fiber yields a gain of 1.443 dB/cm with a slope efficiency >45% for the 100 kHz repetition rate pulses. To further increase the pulse energy, a 1.5 wt% Er-doped phosphate fiber with a core size of 75 μm and a cladding of 250 μm was fabricated [37]. An average output power of 8.5 W at a repetition rate of 4.8 kHz, corresponding to a pulse energy of 1.77 mJ, was obtained with a 28-cm long gain fiber at a pump power of 63 W. Sub-500 fs pulses with a pulse energy of nearly 1 mJ and a peak power of 1.9 GW were obtained after pulse compression.

3. Germanate fiber lasers

Laser sources operating at the 2 μm region are preferred over 1.5 μm Er^{3+} lasers and 1 μm Yb^{3+} and Nd^{3+} lasers for long-range applications, including direct energy laser weapon, LIDAR and sensing systems and direct optical communication, because atmospheric scattering, atmospheric distortion and thermal blooming significantly reduce while increasing the operating wavelength. In addition, 2 μm lasers have found unique applications in nonmetal material processing, especially plastics, highly precise laser surgery and ideal pump sources for high-efficiency mid-infrared or THz laser systems. Although phosphate glasses have shown excellence in making short-length fiber lasers and amplifiers at the 1 μm and 1.55 μm bands, they are not good host material for Tm^{3+} and Ho^{3+} lasers operating at the 2 μm region due to their increased multi-phonon absorption and nonradiative decay. Compared to silica and phosphate glasses, germanate glass has lower phonon energy and longer IR absorption edge. Therefore, Tm^{3+} and Ho^{3+} germanate glass fibers have been fabricated as high-efficiency gain media for fiber laser systems operating at the 2 μm region.

3.1. Single-frequency highly doped germanate fiber lasers

Single-frequency laser sources operating at the 2 μm region are in great demand for various LIDARs. Since germanate glass also displays high RE solubility, highly Tm^{3+}- and Ho^{3+}-doped single-mode germanate glass fibers have been fabricated for the development of DBR single-frequency fiber lasers at 2 μm [38, 39]. A 2-cm long 5 wt% Tm^{3+}-doped germanate fiber with a core diameter of 7 μm and NA of 0.15 was used to develop a single-frequency fiber laser at 1893 nm [38]. As shown in **Figure 11(a)**, this single-frequency fiber laser has a pump threshold of 30 mW, a slope efficiency of 35% and a maximum output power of over 50 mW with respect to the launched power of a single-mode pump laser diode at 805 nm. **Figure 11(b)** shows the output power and optical spectrum (inset) of a 2.05 μm single-frequency fiber laser developed with a 2-cm long 3 wt% Ho^{3+}-doped germanate fiber. This single-frequency Ho^{3+}-doped germanate fiber laser was pumped by a Tm^{3+}-doped fiber laser at 1950 nm. Over 60 mW output power was obtained with the maximum available pump power.

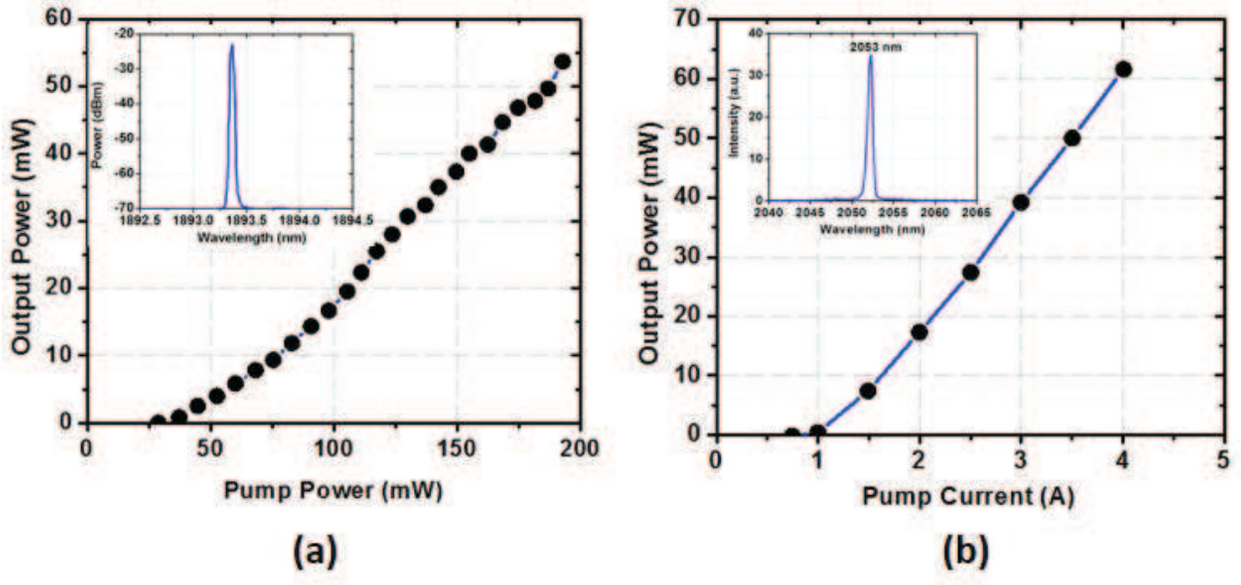

Figure 11. (a) Output power and optical spectrum (inset) of a single-frequency Tm^{3+}-doped germanate fiber laser operating at 1893 nm; (b) output power and optical spectrum (inset) of a single-frequency Ho^{3+}-doped germanate fiber laser operating at 2053 nm.

3.2. High power Tm^{3+}-doped germanate fiber lasers and amplifiers

Tm^{3+} ion is a favorable active element for laser emission at the 2 μm spectral band because of its high quantum efficiency, broad emission band and strong absorption band at 800 nm, where high power and efficiency AlGaAs laser diodes are commercially available. Most importantly, a slope efficiency exceeding the Stokes efficiency can be obtained with Tm^{3+} lasers due to the cross-relaxation energy transfer process ($^3H_6$, $^3H_4 \rightarrow {}^3F_4$, $^3F_4$) between Tm^{3+} ions, which results in a quantum efficiency of 200%. The effect of cross-relaxation energy transfer between Tm^{3+} ions in a germanate glass was verified by the decreased 1.48 μm emission with the increased Tm^{3+} ion concentration [40]. A very high slope efficiency of 58% with respect to the launched power, corresponding to a quantum efficiency of 1.79, was demonstrated with a 4-cm long 4 wt% Tm^{3+}-doped germanate single-mode fiber laser. However, the output power of this single-mode fiber laser is at tens of mW level, which is mainly limited by the available power of single-mode AlGaAs diodes at 800 nm.

In order to develop a high power fiber laser source at 2 μm, highly Tm^{3+}-doped germanate double-cladding fibers with large mode area (LMA) cores were fabricated for cladding-pumping with high power multimode laser diodes [41]. A 64 W fiber laser at 1.9 μm was developed with a 20-cm long 4 wt% Tm^{3+}-doped germanate double-cladding fiber with a core diameter of 50 μm and a NA of 0.02, corresponding to a *V*-number of 1.96. As shown in **Figure 12**, a slope efficiency (SE) of 68% with respect to the launched pump power at 800 nm was demonstrated with single-end pumping configuration, indicating that a quantum efficiency of 1.8 was achieved. As more pump power was launched into the Tm^{3+}-doped germanate fiber by using a dual-end pumping configuration, a 100-W level fiber laser was demonstrated with a 42/200 μm double-cladding fiber, and a slope efficiency of 52.5% was obtained.

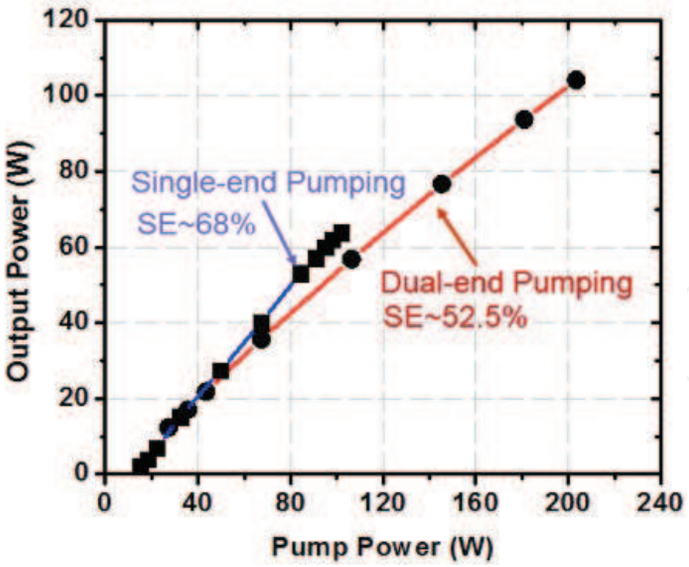

Figure 12. Output power of a single-end pumped 20-cm long 50/200 μm 4 wt% Tm^{3+}-doped germanate fiber laser and of a dual-end pumped 40-cm long 42/200 μm 4 wt% Tm^{3+}-doped germanate fiber laser.

High energy single-frequency pulsed fiber laser sources have also been demonstrated with highly Tm^{3+}-doped germanate fibers [42–44]. In [42], an all-fiber single-frequency Q-switched laser source at 1.92 μm with a pulse energy of 220 μJ was achieved with a monolithic master oscillator and power amplifier (MOPA) configuration. A 2-cm long 5 wt% Tm^{3+}-doped germanate fiber was first used to develop an actively Q-switched single-frequency fiber laser oscillator by using a piezo to press the fiber of the DBR cavity. Tens of ns pulses with tunable width from tens of ns to 300 ns and transform-limited linewidths were obtained. Then, two Tm^{3+}-doped silica fiber amplifiers were used in cascade to increase the pulse energy to 14 μJ. A 20-cm long 4 wt% Tm^{3+}-doped germanate double-cladding fiber with a core diameter of 25 μm and a cladding diameter of 250 μm was used for the last stage of the power amplifier. For 80 ns pulses at a repetition rate of 20 kHz, a pulse energy of 220 μJ, corresponding to a peak power of 2.75 kW, was obtained. **Figure 13(a)** shows the pulse energy and peak power of a power amplifier constituted by a 30-cm long 25/250 μm 4 wt% Tm^{3+}-doped germanate fiber and operating at a repetition rate of 5 kHz for 15 ns pulses [43]. Half-mJ pulses with peak power > 33 kW and negligible nonlinear distortions were obtained at a pump power of 18 W. Single-frequency pulsed fiber laser sources at 1.92 μm with much higher average output power and pulse energy were demonstrated with a 41-cm long 4 wt% Tm^{3+}-doped germanate fiber with a core diameter of 30 μm and a cladding diameter of 300 μm [44]. An average output power of 16 W for single-frequency transform-limited 2.0 ns pulses at a repetition rate of 500 kHz was achieved. As the repetition rate was reduced to 100 kHz, a maximum peak power of 78.1 kW was obtained for the 2 ns pulses. A maximum pulse energy of nearly 1 mJ was achieved at a power of 33 W for 15 ns pulses with a repetition rate of 1 kHz, as shown in **Figure 13(b)**.

Highly Tm^{3+}-doped germanate fibers are also attractive for mode-locked laser power amplifiers with low accumulated nonlinearity because the absorption of such gain fiber is so high and tens of cm long fiber can absorb most of the pump power even with cladding-pumped configurations. A 10 W mode-locked laser source has been developed with a 4 wt% Tm^{3+}-doped

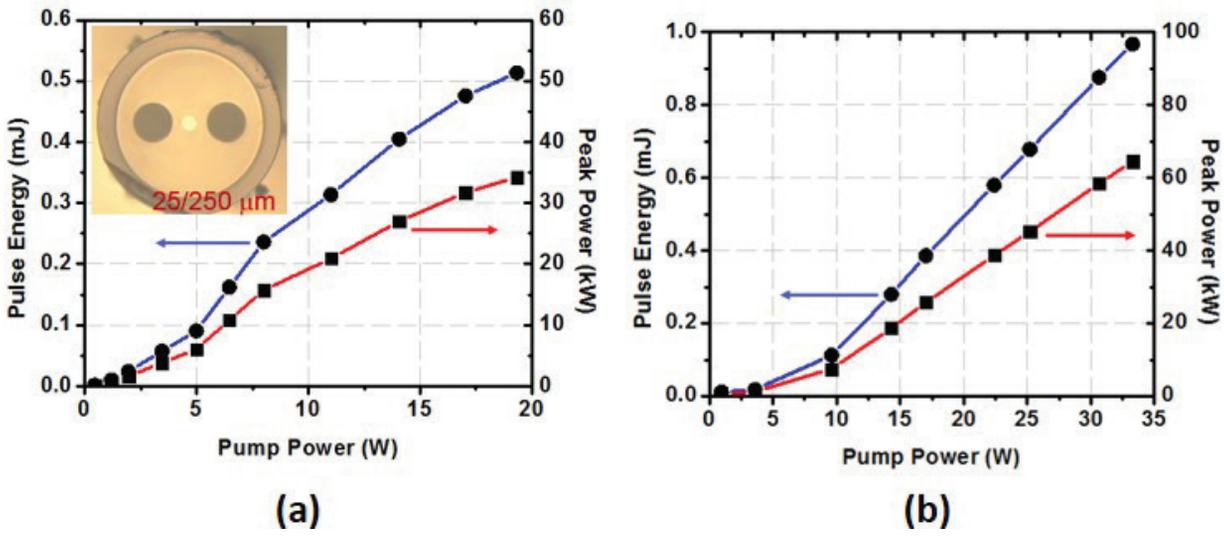

Figure 13. (a) Output pulse energy and peak power of a 25/250 μm 4 wt% Tm-doped germanate fiber amplifier for a 1918.4 nm 5 kHz 15 ns single-frequency laser; (b) output pulse energy and peak power of a 30/300 μm 4 wt% Tm-doped germanate fiber amplifier for a 1918.4 nm 1 kHz 15 ns single-frequency laser.

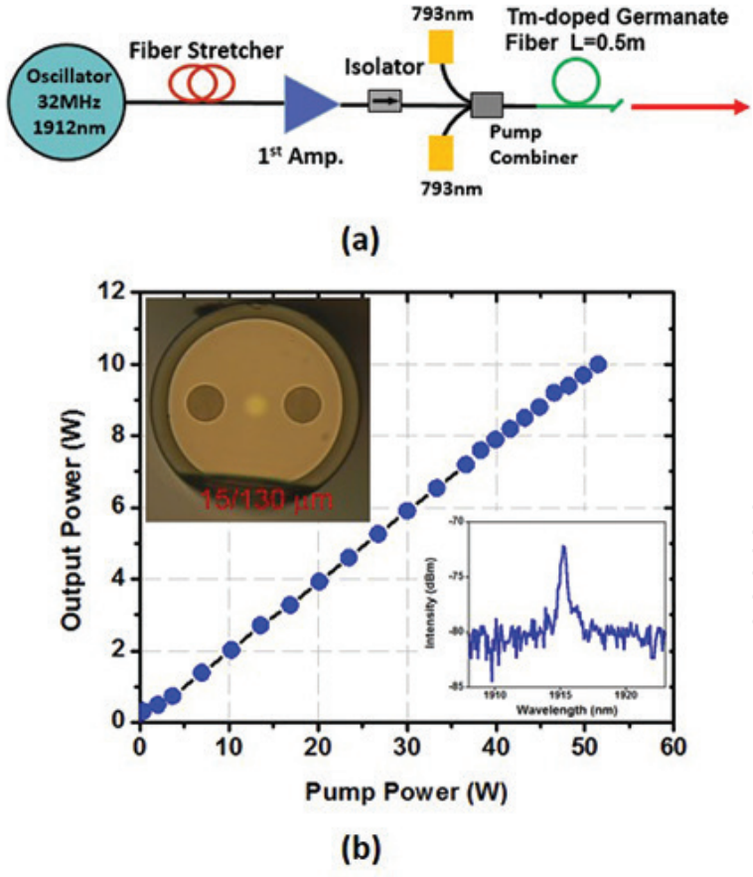

Figure 14. (a) Experimental setup of a 10 W all-fiber mode-locked laser source based on a 15/130 μm 4 wt% Tm^{3+}-doped germanate fiber power amplifier; (b) average output power as a function of the 793 nm pump power of a Tm^{3+}-doped germanate fiber amplifier for 40 ps mode-locked laser at 1920 nm. Insets: Upper left is the microscopic image of the 15/130 μm 4 wt% Tm^{3+}-doped germanate fiber and lower right is the optical spectrum of the mode-locked laser fiber amplifier.

germanate double-cladding fiber with the configuration shown in **Figure 14(a)**. A mode-locked fiber laser oscillator operating at 1912 nm with a repetition rate of 32 MHz was used as the seed laser. The output power of the seed laser was a few mW. A fiber stretcher was used to stretch the pulse width to 40 ps. A core-pumped Tm^{3+}-doped silica fiber amplifier was used to increase the mode-locked laser power to 150 mW first. Then, a 50-cm long Tm^{3+}-doped germanate double-cladding fiber with a core diameter of 15 μm and a cladding of 130 μm was used for the power amplifier stage. The output power of the Tm^{3+}-doped germanate fiber amplifier as a function of the pump is shown in **Figure 14(b)**. Over 10 W output power with a slope efficiency of 20% was obtained at a pump power of 50 W. The optical spectrum of the 10 W mode-locked laser fiber amplifier is shown in the lower right inset. The spectrum broadening and distortion due to the accumulated nonlinear effects are negligible. The efficiency of the Tm^{3+}-doped germanate fiber amplifier is lower than that of a Tm^{3+}-doped silica fiber amplifier. It can be improved by optimizing the composition of the germanate glass to significantly enhance the cross-relaxation process and reduce the fiber propagation loss.

4. Tellurite fiber lasers

Compared to phosphate and germanate glasses, tellurite glass displays a lower maximum phonon energy (800 cm^{-1}) that allows the transmission of light further into the mid-infrared (up to ~5 μm) [45]. In addition, tellurite glass has large rare-earth ion solubility and enhanced absorption and emission cross-sections due to the large refractive index of ~2.0, making rare-earth-doped tellurite glasses very attractive materials for efficient laser emission. So far, various rare-earth-doped fiber lasers at the 1, 1.6 and 2 μm wavelength regions have been reported [46–55]. On the other hand, tellurite glass has large nonlinear refractive index (5.9×10^{-19} m^2/W), high thermal stability and strong corrosion resistance, making tellurite fiber an ideal medium for nonlinear wavelength conversion. So far, nonlinear wavelength conversion lasers including SBS lasers, Raman lasers and supercontinuum lasers have been studied and investigated with tellurite fibers [56–66].

4.1. Rare-earth-doped tellurite fiber lasers

The first laser emission with a rare-earth-doped tellurite fiber was demonstrated in 1994 [46]. A single-mode Nd^{3+}-doped tellurite fiber with an elliptical core of 3 μm × 6.5 μm and a NA of 0.21 was fabricated with the rod-in-tube technique. A single-mode laser emission with a lasing threshold of 27 mW was observed at 1061 nm. A slope efficiency of 23% was obtained with 11.9% Fresnel reflection at both ends of the fiber cavity. An Er^{3+}-doped tellurite fiber laser was first reported by Mori et al. in 1997 [47]. A maximum output power of 2.5 mW at 1560 nm with a slope efficiency of 0.65% was obtained at a pump power of 500 mW. Afterwards, Er^{3+}-doped tellurite fiber amplifiers were studied and investigated for the L-band signal amplification for optical communications [48, 49]. Since Er^{3+}-doped tellurite glass has a large emission cross-section due to the electric dipole moment transition with a large refractive index, expressed by $\sigma_e \sim (n^2 + 2)^2/9n$, a small signal gain exceeding 20 dB over a bandwidth as wide as 80 nm including the 1.55 μm and 1.58 μm bands can be obtained with an Er^{3+}-doped tellurite fiber amplifier. Most importantly, the Er^{3+}-doped tellurite fiber amplifier was found to be very suitable for the

L-band signal amplification especially for signal wavelengths beyond 1600 nm [49]. In addition to the Er^{3+}-doped tellurite fiber for the L-band signal amplification, the S-band signal amplification was demonstrated with a 0.4 mol% Tm^{3+}-doped tellurite fiber by using the transition from $^3H_4$ to $^3F_4$ levels of Tm^{3+} ions [50]. A fiber-to-fiber gain of 11 dB and an internal gain of 35 dB were achieved with a dual-end pumping configuration.

Compared to the S-band signal amplification, the Tm^{3+}-doped tellurite fiber has attracted more attention for laser emission at the 2 μm band. In 2008, Richards et al. reported a high-efficiency Tm^{3+}-doped tellurite fiber laser at 1.88–1.99 μm [51]. An output power of 280 mW with a slope efficiency of 76% was obtained with a 32-cm long 1 wt% Tm^{3+}-doped tellurite fiber core pumped by a silica fiber laser at 1.6 μm. A more powerful output at 2 μm was obtained by cladding-pumping with a multimode laser diode at 800 nm [52]. An output power of 1.12 W with a slope efficiency of 20% was achieved with a 40-cm long 1 wt% Tm^{3+}-doped tellurite double-cladding fiber. Since Ho^{3+} ions are characterized by a larger emission peak than Tm^{3+} ions and Ho^{3+} ions can be excited via an energy transfer process between the Tm^{3+} and Ho^{3+} ions, the sensitization of Ho^{3+} by Tm^{3+} has been usually exploited to achieve laser emission beyond 2 μm by taking advantage of the high absorption of Tm^{3+} ions at 800 nm. In [53], a 2.1 μm fiber laser with an output power of 35 mW was demonstrated with a 7 cm long 1 mol% Tm^{3+} and 0.5 mol% Ho^{3+} co-doped tellurite double-cladding fiber. This fiber was fabricated with the rod-in-tube method and has a core diameter of 9 μm and a NA of 0.14. In [54], a high-efficiency Tm^{3+}/Ho^{3+} co-doped tellurite fiber laser at 2.1 μm was demonstrated with in-band pumping at 1.6 μm. A continuous-wave output power of 160 mW with a slope efficiency of 62% was obtained at a pump power of 350 mW. In addition to Tm^{3+} ions, Yb^{3+} ions were also added as sensitizer to enhance the pump absorption of a Ho^{3+} laser system. A tellurite fiber with a 7.5 μm core doped with 1.5 wt% Yb_2O_3, 1.0 wt% Tm_2O_3 and 1.0 wt% Ho_2O_3 was fabricated [55]. A 60 mW laser output at 2.1 μm with a slope efficiency of 25% was demonstrated with a 17-cm long $Tm^{3+}/Ho^{3+}/Yb^{3+}$ triply-doped tellurite fiber. Although high-efficiency Tm^{3+}-, Tm^{3+}/Ho^{3+}- and $Tm^{3+}/Ho^{3+}/Yb^{3+}$-doped tellurite fiber lasers at 2 μm have been demonstrated, their output is still much lower than that of germanate and silica fiber lasers. Higher output power tellurite fiber lasers can be obtained by reducing the propagation loss of the fiber and improving the thermal management of the fiber laser.

4.2. Nonlinear wavelength conversion tellurite fiber lasers

Because of its broad transmission and large nonlinearity, tellurite glass has been extensively used as a low phonon energy oxide glass in nonlinear photonic devices. Combining the long interaction length and small core size with large nonlinearity, undoped tellurite glass fibers are excellent platforms for nonlinear wavelength conversion lasers with low threshold and high efficiency.

The SBS can convert the incident pump light into lower energy scattered light in counter-propagating direction due to the interaction of the pump light and acoustic phonons. The SBS has found applications in optical amplification, optical fiber sensors, phase conjugation and slow light generation. A SBS laser based on tellurite fiber was first demonstrated with a 200-m long single-mode tellurite fiber with a core diameter of 2.2 μm [56]. A maximum unsaturated power of 54.6 mW at 1550 nm with a slope efficiency of 38.2% was achieved, and the Brillouin gain coefficient of the tellurite fiber was measured to be 1.6989×10^{-10} m/W.

Compared to the Brillouin scattering, the Raman scattering is more attractive for optical amplification and nonlinear wavelength conversion because the Raman gain bandwidth and frequency shift are much larger than those of the Brillouin scattering. By taking advantage of the large Raman gain coefficient (55 W^{-1}/km), broad gain bandwidth (~300 cm^{-1}) and large Raman shift (~750 cm^{-1}) of the tellurite fiber, Mori et al. demonstrated a tellurite fiber Raman amplifier with a gain of over 10 dB and a noise figure below 10 dB from 1490 to 1650 nm [57]. Qin et al. reported a widely tunable ring-cavity tellurite fiber Raman laser with more than 100 nm tunable range (1495–1600 nm) [58]. In [59], Raman tellurite fiber lasers operating at 3–5 μm pumped by readily available CW and Q-switched Er^{3+}-doped fluoride fiber lasers at 2.8 μm were proposed and numerically investigated. The simulation results showed that watt level or even 10-W level fiber laser sources in the 3–5 μm atmospheric transparency window can be achieved by utilizing the first- and second-order Raman scattering in the tellurite fiber. Raman scattering can also be utilized to achieve widely wavelength tunable ultrashort pulses through the soliton self-frequency shift (SSFS), which originates from the intra-pulse stimulated Raman scattering that transfers the high frequency part of the pulse spectrum to the low frequency part. In [60], a widely wavelength tunable 100 fs pulsed laser source in the 1.6–2.65 μm range was achieved with a suspended core microstructured tellurite fiber pumped by a hybrid Er^{3+}/Tm^{3+}-doped silica fiber system.

Supercontinuum (SC) laser sources possessing ultra-broad spectral bandwidth and extremely high spectral brightness have found a variety of applications. Optical fibers have been considered as an inherently excellent candidate for SC generation because they can provide a significant length and guide small beam size for the nonlinear interaction. Because of the large nonlinearity and broad transmission bandwidth, tellurite fibers have shown advantages in SC generation with a low pump power threshold and a very broad spectral bandwidth [61–66]. In 2008, a broadband supercontinuum light spanning over 789–4870 nm was demonstrated with an 8-mm long microstructured tellurite fiber [61]. This tellurite fiber has a core diameter of 2.5 μm, a nonlinear waveguide coefficient of 596 W^{-1}/km and a zero-dispersion wavelength (ZDW) of 1380 nm, allowing anomalous dispersion pumping at 1550 nm. An average power of 70 mW was obtained at a launched pump power of 150 mW. In [62], in order to generate flattened SC light, a microstructured tellurite fiber was tapered to tailor the group velocity dispersion from a small positive value to a large negative one. A flattened SC laser spanning from 843 to 2157 nm with less than 10 dB intensity variation was demonstrated with a 5 -cm long and zero-dispersion-decreasing microstructured tellurite fiber. In addition to the SC generation, the second and third harmonic generations in microstructured tellurite fibers were investigated with a 1557 nm femtosecond fiber laser [63]. Supercontinuum light spanning over 470–2400 nm was achieved with a microstructured tellurite fiber with a core diameter of 2.7 μm. This research demonstrated that the chromatic dispersion controlled microstructured tellurite fibers are potential candidates for second harmonic generation, third harmonic generation and SC generation expanding from visible to mid-IR regions. SC generation in highly nonlinear microstructured tellurite fibers pumped by a CW/quasi-CW laser was investigated by Liao et al. [64]. SC with spectral bandwidth broader than one

octave was achieved with a sub-meter fiber and a watt-level peak-power pump. However, these SC laser sources are based on microstructured tellurite fibers, which usually have a very small effective core area and poor heat dissipation capability, and thus their output power scaling is constrained by the breakdown damage of the fiber cores. To achieve a high average power SC laser, solid-cladding tellurite fibers have to be used due to the improved thermal and mechanical properties.

The ZDW of a tellurite glass is typically around 2.3 μm, so the zero dispersion wavelength of a regular step-index tellurite fiber is longer than 2.3 μm. It is worthwhile noting that this value is not compatible with the pump wavelength of the most commonly available high power pump sources, thus making it challenging to achieve high power SC with broad spectral bandwidth. To overcome this constraint, a solid-cladding tellurite fiber with a W-type index profile as the one shown in the inset of **Figure 15(b)** was fabricated by the rod-in-tube method. This fiber has a solid core with a diameter of 3.8 μm and an 11.4 μm inner cladding with index lower than that of the core and the outer cladding. The dispersion of the W-type index fiber was measured and is shown in the inset of **Figure 15(c)**. The first zero-dispersion wavelength is shifted to 2 μm and there is another zero-dispersion wavelength at 3.9 μm. This fiber has been used to demonstrate the first watt-level SC laser source based on a tellurite fiber [65]. More than 1.2 W SC were obtained with conversion efficiency greater than 30% from the 1.9 μm pump wavelength to the 2–5 μm spectral range. Detailed experimental parameters study on mid-IR SC generation in W-type index tellurite fibers is reported in [66]. Soliton SC with a maximum spectral width of over 2000 nm spanning from 2.6 to 4.6 μm and output powers of up to 160 mW was obtained with a 4.2 μm core fiber pumped at 3 μm. The power scaling of the SC generation based on the W-type index tellurite fiber was demonstrated with the all-fiber setup shown in **Figure 15(a)**. A mode-locked fiber laser at 1912 nm with a repetition rate of 32 MHz was used as the seed laser. The pulse width is stretched to 40 ps by a fiber stretcher. The average power of the mode-locked laser was increased to over 10 W by three-stage Tm^{3+}-doped fiber amplifiers. The 10 W mode-locked laser was coupled into the W-type index tellurite fiber via a fiber mode-field adapter. The output power of the all-fiber SC laser source was measured and is shown in **Figure 15(b)**. Nearly 5 W SC were generated at the pump power of 10.6 W. The optical spectrum of the SC laser source is shown in **Figure 15(c)**. The power intensity at long wavelength starts to decrease at about 3.8 μm, which is close to the second zero-dispersion wavelength. Red-shift dispersion waves were measured at wavelengths beyond 4 μm. The long wavelength of the SC can be further extended by using a tellurite fiber with a longer second zero-dispersion wavelength. High power mid-infrared SC laser sources with a high spectral power density in the 3–5 μm atmospheric window are very attractive for long distance applications. Both simulation and experimental results have confirmed that SC with a very high power proportion in the 3–5 μm region can be obtained with a tellurite fiber pumped by ultrafast mid-infrared pulses at a wavelength of around 3 μm [66, 67]. Various Q-switched and mode-locked fiber lasers at 3 μm have already been demonstrated [68, 69]. Therefore, high power all-fiber SC laser sources with >90% power intensity in the atmospheric window can be developed with current fiber laser technology.

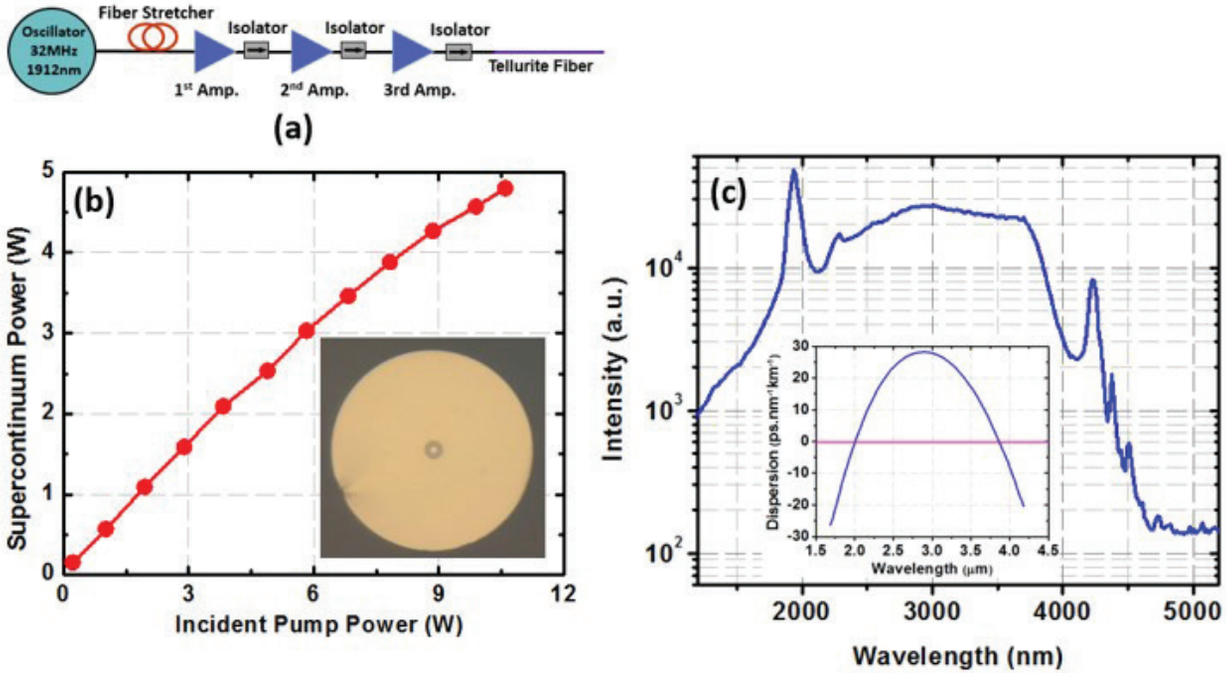

Figure 15. (a) Experimental setup of a 5 W all-fiber SC laser source based on a W-type index tellurite fiber. (b) Average output power of the SC laser source as a function of the mode-locked pump power at 1920 nm. Inset: microscope image of the W-type index tellurite fiber. (c) Optical spectrum of the 5 W all-fiber SC laser source. Inset: Measured dispersion of the W-type index tellurite fiber.

Author details

Xiushan Zhu[1], Arturo Chavez-Pirson[2], Daniel Milanese[3,6]*, Joris Lousteau[4], Nadia Giovanna Boetti[5], Diego Pugliese[3] and Nasser Peyghambarian[1,2]

*Address all correspondence to: daniel.milanese@polito.it

1 College of Optical Sciences, University of Arizona, Tucson, AZ, United States of America

2 NP Photonics Inc., Tucson, AZ, United States of America

3 Department of Applied Science and Technology and RU INSTM, Politecnico di Torino, Torino, Italy

4 Optoelectronics Research Centre, University of Southampton, Southampton, United Kingdom

5 Istituto Superiore Mario Boella, Torino, Italy

6 Consiglio Nazionale delle Ricerche, Istituto di Fotonica e Nanotecnologie, Trento, Italy

References

[1] Yamane M, Asahara Y. Glasses for Photonics. 1st ed. Cambridge, UK: Cambridge University Press; 2004. 282 p

[2] Digonnet MJF, editor. Rare-Earth-Doped Fiber Lasers and Amplifiers. 1st ed. Boca Raton, FL, USA: CRC Press; 2001. 798 p

[3] Richardson DJ, Nilsson J, Clarkson WA. High power fiber lasers: Current status and future perspectives. Journal of the Optical Society of America B: Optical Physics. 2010; **27**:B63-B92. DOI: 10.1364/JOSAB.27.000B63

[4] Dudley JM, Taylor JR, editors. Supercontinuum Generation in Optical Fibers. 1st ed. Cambridge, UK: Cambridge University Press; 2010. 419 p. DOI: 10.1017/CBO9780511750465

[5] Brawer SA, White WB. Raman spectroscopic investigation of the structure of silicate glasses. I. The binary alkali silicates. The Journal of Chemical Physics. 1975;**63**:2421-2432. DOI: 10.1063/1.431671

[6] Quimby RS, Miniscalco WJ, Thompson B. Clustering in erbium-doped silica glass fibers analyzed using 980 nm excited-state absorption. Journal of Applied Physics. 1994; **76**:4472-4478. DOI: 10.1063/1.357278

[7] Kitamura R, Pilon L, Jonasz M. Optical constants of silica glass from extreme ultraviolet to far infrared at near room temperature. Applied Optics. 2007;**46**:8118-8133. DOI: 10.1364/AO.46.008118

[8] Charschan SS. In the beginning there was ANSI Z136.1. Journal of Laser Applications. 1997;**9**:189-195. DOI: 10.2351/1.4745459

[9] Yamashita Y. Nd- and Er-doped phosphate glass for fiber laser. In: Proceedings of SPIE 1171, Fiber Laser Sources and Amplifiers; 5-7 September 1989; Boston. Bellingham, WA, USA: SPIE; 1990. pp. 291-297

[10] Griebner U, Koch R, Schönnagel H, Grunwald R. Efficient laser operation with nearly diffraction-limited output from a diode-pumped heavily Nd-doped multimode fiber. Optics Letters. 1996;**21**:266-268. DOI: 10.1364/OL.21.000266

[11] Wu R, Myers JD, Myers MJ, Hardy CR. Nd-doped cladding pumped fiber laser. In: Proceedings of the Fiber Optics and Communication Technologies, Optics in the Southeast; November 4-5, 2001; Charlotte, Washington, USA: OSA; 2001. pp. 1-5

[12] Zhang G, Wang M, Yu C, Zhou Q, Qiu J, Hu L, Chen D. Efficient generation of watt-level output from short-length Nd-doped phosphate fiber lasers. IEEE Photonics Technology Letters. 2011;**23**:350-352. DOI: 10.1109/LPT.2010.2103306

[13] Lee Y-W, Digonnet MJF, Sinha S, Urbanek KE, Byer RL, Jiang S. High-power Yb^{3+}-doped phosphate fiber amplifier. IEEE Journal of Selected Topics in Quantum Electronics. 2009;**15**:93-102. DOI: 10.1109/JSTQE.2008.2010263

[14] Hwang B-C, Jiang S, Luo T, Seneschal K, Sorbello G, Morrell M, Smektala F, Honkanen S, Lucas J, Peyghambarian N. Performance of high-concentration Er^{3+}-doped phosphate fiber amplifiers. IEEE Photonics Technology Letters. 2001;**13**:197-199. DOI: 10.1109/68.914319

[15] Boetti NG, Scarpignato GC, Lousteau J, Pugliese D, Bastard L, Broquin J-E, Milanese D. High concentration Yb-Er co-doped phosphate glass for optical fiber amplification. Journal of Optics. 2015;**17**:065705. DOI: 10.1088/2040-8978/17/6/065705

[16] Qiu T, Li L, Schülzgen A, Temyanko VL, Luo T, Jiang S, Mafi A, Moloney JV, Peyghambarian N. Generation of 9.3-W multimode and 4-W single-mode output from 7-cm short fiber lasers. IEEE Photonics Technology Letters. 2004;**16**:2592-2594. DOI: 10.1109/LPT.2004.836352

[17] Li L, Morrell M, Qiu T, Temyanko VL, Schülzgen A, Mafi A, Kouznetsov D, Moloney JV, Luo T, Jiang S, Peyghambarian N. Short cladding-pumped Er/Yb phosphate fiber laser with 1.5 W output power. Applied Physics Letters. 2004;**85**:2721-2723. DOI: 10.1063/1.1798394

[18] Li L, Schülzgen A, Temyanko VL, Qiu T, Morrell MM, Wang Q, Mafi A, Moloney JV, Peyghambarian N. Short-length microstructured phosphate glass fiber lasers with large mode areas. Optics Letters. 2005;**30**:1141-1143. DOI: 10.1364/OL.30.001141

[19] Spiegelberg C, Geng J, Hu Y, Kaneda Y, Jiang S, Peyghambarian N. Low-noise narrow-linewidth fiber laser at 1550 nm (June 2003). Journal of Lightwave Technology. 2004; **22**:57-62. DOI: 10.1109/JLT.2003.822208

[20] Hofmann P, Voigtländer C, Nolte S, Peyghambarian N, Schülzgen A. 550-mW output power from a narrow linewidth all-phosphate fiber laser. Journal of Lightwave Technology. 2013;**31**:756-760. DOI: 10.1109/JLT.2012.2233392

[21] Qiu T, Suzuki S, Schülzgen A, Li L, Polynkin A, Temyanko VL, Moloney JV, Peyghambarian N. Generation of watt-level single-longitudinal-mode output from cladding-pumped short fiber lasers. Optics Letters. 2005;**30**:2748-2750. DOI: 10.1364/OL.30.002748

[22] Xu S, Yang Z, Zhang W, Wei X, Qian Q, Chen D, Zhang Q, Shen S, Peng M, Qiu J. 400 mW ultrashort cavity low-noise single-frequency Yb^{3+}-doped phosphate fiber laser. Optics Letters. 2011;**36**:3708-3710. DOI: 10.1364/OL.36.003708

[23] Leigh M, Shi W, Zong J, Wang J, Jiang S, Peyghambarian N. Compact, single-frequency all-fiber Q-switched laser at 1 μm. Optics Letters. 2007;**32**:897-899. DOI: 10.1364/OL.32.000897

[24] Yang C, Zhao Q, Feng Z, Peng M, Yang Z, Xu S. 1120 nm kHz-linewidth single-polarization single-frequency Yb-doped phosphate fiber laser. Optics Express. 2016;**24**:29794-29799. DOI: 10.1364/OE.24.029794

[25] Zhu X, Zhu G, Shi W, Zong J, Wiersma K, Nguyen D, Norwood RA, Chavez-Pirson A, Peyghambarian N. 976 nm single-polarization single frequency ytterbium-doped phosphate fiber amplifiers. IEEE Photonics Technology Letters. 2013;**25**:1365-1368. DOI: 10.1109/LPT.2013.2266113

[26] Wu J, Zhu X, Temyanko V, LaComb L, Kotov L, Kiersma K, Zong J, Chavez-Pirson A, Norwood RA, Peyghambarian N. Yb^{3+}-doped double-clad phosphate fiber for 976 nm single-frequency laser amplifiers. Optical Materials Express. 2017;**7**:1310-1316. DOI: 10.1364/OME.7.001310

[27] Yamashita S, Yoshida T, Set SY, Polynkin P, Peyghambarian N. Passively mode-locked short-cavity 10 GHz Er:Yb-codoped phosphate-fiber laser using carbon nanotubes. In:

Proceedings of SPIE 6453, Fiber Lasers IV: Technology, Systems, and Applications; January 20-25, 2007; San Jose. Bellingham, WA, USA: SPIE; 2007. p. 64531Y

[28] Thapa R, Nguyen D, Zong J, Chavez-Pirson A. All-fiber fundamentally mode-locked 12 GHz laser oscillator based on an Er/Yb-doped phosphate glass fiber. Optics Letters. 2014;**39**:1418-1421. DOI: 10.1364/OL.39.001418

[29] Lee YW, Sinha S, Digonnet MJF, Byer RL. 20 W single-mode Yb^{3+}-doped phosphate fiber laser. Optics Letters. 2006;**31**:3255-3257. DOI: 10.1364/OL.31.003255

[30] Leigh M, Shi W, Zong J, Yao Z, Jiang S, Peyghambarian N. High peak power single frequency pulses using a short polarization-maintaining phosphate glass fiber with a large core. Applied Physics Letters. 2008;**92**:181108. DOI: 10.1063/1.2917470

[31] Shi W, Petersen EB, Leigh M, Zong J, Yao Z, Chavez-Pirson A, Peyghambarian N. High SBS-threshold single-mode single-frequency monolithic pulsed fiber laser in the C-band. Optics Express. 2009;**17**:8237-8245. DOI: 10.1364/OE.17.008237

[32] Shi W, Leigh MA, Zong J, Yao Z, Nguyen DT, Chavez-Pirson A, Peyghambarian N. High-power all-fiber-based narrow-linewidth single-mode fiber laser pulses in the C-band and frequency conversion to THz generation. IEEE Journal of Selected Topics in Quantum Electronics. 2009;**15**:377-384. DOI: 10.1109/JSTQE.2008.2010234

[33] Akbulut M, Miller A, Wiersma K, Zong J, Rhonehouse D, Nguyen D, Chavez-Pirson A. High energy, high average and peak power phosphate-glass fiber amplifiers for 1 micron band. In: Proceedings of SPIE 8961, Fiber Lasers XI: Technology, Systems, and Applications; February 1-6, 2014; San Francisco. Bellingham, WA, USA: SPIE; 2014. p. 89611X

[34] Shi W, Peterson EB, Yao Z, Nguyen DT, Zong J, Stephen MA, Chavez-Pirson A, Peyghambarian N. Kilowatt-level stimulated-Brillouin-scattering-threshold monolithic transform-limited 100 ns pulsed fiber laser at 1530 nm. Optics Letters. 2010;**35**:2418-2420. DOI: 10.1364/OL.35.002418

[35] Polynkin P, Polynkin A, Panasenko D, Peyghambarian N, Moloney JV. All-fiber picosecond laser system at 1.5 μm based on amplification in short and heavily doped phosphate-glass fiber. IEEE Photonics Technology Letters. 2006;**18**:2194-2196. DOI: 10.1109/LPT.2006.884242

[36] Peng X, Kim K, Mielke M, Jennings S, Masor G, Stohl D, Chavez-Pirson A, Nguyen DT, Rhonehouse D, Zong J, Churin D, Peyghambarian N. High efficiency, monolithic fiber chirped pulse amplification system for high energy femtosecond pulse generation. Optics Express. 2013;**21**:25440-25451. DOI: 10.1364/OE.21.025440

[37] Peng X, Kim K, Mielke M, Jennings S, Masor G, Stohl D, Chavez-Pirson A, Nguyen DT, Rhonehouse D, Zong J, Churin D, Peyghambarian N. Monolithic fiber chirped pulse amplification system for millijoule femtosecond pulse generation at 1.55 μm. Optics Express 2014;**22**:2459-2464. DOI: 10.1364/OE.22.002459

[38] Geng J, Wu J, Jiang S, Yu J. Efficient operation of diode-pumped single-frequency thulium-doped fiber lasers near 2 μm. Optics Letters. 2007;**32**:355-357. DOI: 10.1364/OL.32.000355

[39] Wu J, Yao Z, Zong J, Chavez-Pirson A, Peyghambarian N, Yu J. Single-frequency fiber laser at 2.05 μm based on Ho-doped germanate glass fiber. In: Proceedings of SPIE 7195, Fiber Lasers VI: Technology, Systems, and Applications; January 24-29, 2009; San Jose. Bellingham, WA, USA: SPIE; 2009. p. 71951K

[40] Wu J, Jiang S, Luo T, Geng J, Peyghambarian N, Barnes NP. Efficient thulium-doped 2-μm germanate fiber laser. IEEE Photonics Technology Letters 2006;**18**:334-336. DOI: 10.1109/LPT.2005.861970

[41] Wu J, Yao Z, Zong J, Jiang S. Highly efficient high-power thulium-doped germanate glass fiber laser. Optics Letters. 2007;**32**:638-640. DOI: 10.1364/OL.32.000638

[42] Shi W, Petersen EB, Nguyen DT, Yao Z, Chavez-Pirson A, Peyghambarian N, Yu J. 220 μJ monolithic single-frequency Q-switched fiber laser at 2 μm by using highly Tm-doped germanate fibers. Optics Letters 2011;**36**:3575-3577. DOI: 10.1364/OL.36.003575

[43] Fang Q, Shi W, Peterson E, Kieu K, Chavez-Pirson A, Peyghambarian N. Half-mJ all-fiber-based single-frequency nanosecond pulsed fiber laser at 2-μm. IEEE Photonics Technology Letters 2012;**24**:353-355. DOI: 10.1109/LPT.2011.2178824

[44] Fang Q, Shi W, Kieu K, Petersen E, Chavez-Pirson A, Peyghambarian N. High power and high energy monolithic single frequency 2 μm nanosecond pulsed fiber laser by using large core Tm-doped germanate fibers: experiment and modeling. Optics Express 2012;**20**:16410-16420. DOI: 10.1364/OE.20.016410

[45] Rhonehouse DL, Zong J, Nguyen D, Thapa R, Wiersma K, Smith C, Chavez-Pirson A. Low loss, wide transparency, robust tellurite glass fibers for mid-IR (2-5 μm) applications. In: Proceedings of SPIE 8898, Technologies for Optical Countermeasures X and High-Power Lasers 2013: Technology and Systems; September 23-26, 2013; Dresden. Bellingham, WA, USA: SPIE; 2013. p. 88980D

[46] Wang JS, Machewirth DP, Wu F, Snitzer E, Vogel EM. Neodymium-doped tellurite single-mode fiber laser. Optics Letters. 1994;**19**:1448-1449. DOI: 10.1364/OL.19.001448

[47] Mori A, Ohishi Y, Sudo S. Erbium-doped tellurite glass fibre laser and amplifier. Electronics Letters. 1997;**33**:863-864. DOI: 10.1049/el:19970585

[48] Mori A, Sakamoto T, Shikano K, Kobayashi K, Hoshino K, Shimizu M. Gain flattened Er^{3+}-doped tellurite fibre amplifier for WDM signals in the 1581-1616 nm wavelength region. Electronics Letters. 2000;**36**:621-622. DOI: 10.1049/el:20000504

[49] Mori A, Sakamoto T, Kobayashi K, Shikano K, Oikawa K, Hoshino K, Kanamori T, Ohishi Y, Shimizu M. 1.58-μm broad-band erbium-doped tellurite fiber amplifier. Journal of Lightwave Technology 2002;**20**:822-827. DOI: 10.1109/JLT.2002.1007935

[50] Taylor ERM, Ng LN, Nilsson J, Caponi R, Pagano A, Potenza M, Sordo B. Thulium-doped tellurite fiber amplifier. IEEE Photonics Technology Letters. 2004;**16**:777-779. DOI: 10.1109/LPT.2004.823733

[51] Richards B, Tsang Y, Binks D, Lousteau J, Jha A. Efficient ~2 μm Tm^{3+}-doped tellurite fiber laser. Optics Letters. 2008;**33**:402-404. DOI: 10.1364/OL.33.000402

[52] Li K, Zhang G, Hu L. Watt-level ~2 μm laser output in Tm^{3+}-doped tungsten tellurite glass double-cladding fiber. Optics Letters 2010;**35**:4136-4138. DOI: 10.1364/OL.35.004136

[53] Li K, Zhang G, Wang X, Hu L, Kuan P, Chen D, Wang M. Tm^{3+} and Tm^{3+}-Ho^{3+} co-doped tungsten tellurite glass single mode fiber laser. Optics Letters. 2012;**20**:10115-10121. DOI: 10.1364/OE.20.010115

[54] Tsang Y, Richards B, Binks D, Lousteau J, Jha A. Tm^{3+}/Ho^{3+} codoped tellurite fiber laser. Optics Letters. 2008;**33**:1282-1284. DOI: 10.1364/OL.33.001282

[55] Tsang Y, Richards B, Binks D, Lousteau J, Jha AA. Yb^{3+}/Tm^{3+}/Ho^{3+} triply-doped tellurite fibre laser. Optics Express. 2008;**16**:10690-10695. DOI: 10.1364/OE.16.010690

[56] Qin G, Mori A, Ohishi Y. Brillouin lasing in a single-mode tellurite fiber. Optics Letters. 2007;**32**:2179-2181. DOI: 10.1364/OL.32.002179

[57] Mori A, Masuda H, Shikano K, Shimizu M. Ultra-wide-band tellurite-based fiber Raman amplifier. Journal of Lightwave Technology. 2003;**21**:1300-1306. DOI: 10.1109/JLT.2003.810917

[58] Qin G, Liao M, Suzuki T, Mori A, Ohishi Y. Widely tunable ring-cavity tellurite fiber Raman laser. Optics Letters. 2008;**33**:2014-2016. DOI: 10.1364/OL.33.002014

[59] Zhu G, Geng L, Zhu X, Li L, Chen Q, Norwood RA, Manzur T, Peyghambarian N. Towards ten-watt-level 3-5 μm Raman lasers using tellurite fiber. Optics Express. 2015;**23**:7559-7573. DOI: 10.1364/OE.23.007559

[60] Koptev MY, Anashkina EA, Andrianov AV, Dorofeev VV, Kosolapov AF, Muravyev SV, Kim AV. Widely tunable mid-infrared fiber laser source based on soliton self-frequency shift in microstructured tellurite fiber. Optics Letters. 2015;**40**:4094-4097. DOI: 10.1364/OL.40.004094

[61] Domachuk P, Wolchover NA, Cronin-Golomb M, Wang A, George AK, Cordeiro CMB, Knight JC, Omenetto FG. Over 4000 nm bandwidth of mid-IR supercontinuum generation in sub-centimeter segments of highly nonlinear tellurite PCFs. Optics Express. 2008;**16**:7161-7168. DOI: 10.1364/OE.16.007161

[62] Qin G, Yan X, Kito C, Liao M, Suzuki T, Mori A, Ohishi Y. Zero-dispersion-wavelength-decreasing tellurite microstructured fiber for wide and flattened supercontinuum generation. Optics Letters. 2010;**35**:136-138. DOI: 10.1364/OL.35.000136

[63] Qin G, Liao M, Chaudhari C, Yan X, Kito C, Suzuki T, Ohishi Y. Second and third harmonics and flattened supercontinuum generation in tellurite microstructured fibers. Optics Letters. 2010;**35**:58-60. DOI: 10.1364/OL.35.000058

[64] Liao M, Gao W, Duan Z, Yan X, Suzuki T, Ohishi Y. Supercontinuum generation in short tellurite microstructured fibers pumped by a quasi-cw laser. Optics Letters. 2012;**37**:2127-2129. DOI: 10.1364/OL.37.002127

[65] Thapa R, Rhonehouse D, Nguyen D, Wiersma K, Smith C, Zong J, Chavez-Pirson A. Mid-IR supercontinuum generation in ultra-low loss, dispersion-zero shifted tellurite glass fiber with extended coverage beyond 4.5 μm. In: Proceedings of SPIE 8898, Technologies for Optical Countermeasures X and High-Power Lasers 2013: Technology and Systems; September 23-26, 2013; Dresden. Bellingham, WA, USA: SPIE; 2013. p. 889808

[66] Kedenburg S, Steinle T, Mörz F, Steinmann A, Nguyen D, Rhonehouse D, Zong J, Chavez-Pirson A, Giessen H. Soliton supercontinuum of femtosecond mid-IR pulses in W-type index tellurite fibers with two zero dispersion wavelengths. APL Photonics. 2016;**1**:086101. DOI: 10.1063/1.4958333

[67] Wei C, Zhu X, Norwood RA, Song F, Peyghambarian N. Numerical investigation on high power mid-infrared supercontinuum fiber lasers pumped at 3 μm. Optics Express. 2013;**21**:29488-29504. DOI: 10.1364/OE.21.029488

[68] Wei C, Zhu X, Norwood RA, Peyghambarian N. Passively continuous-wave mode-locked Er^{3+}-doped ZBLAN fiber laser at 2.8 μm. Optics Letters. 2012;**37**:3849-3851. DOI: 10.1364/OL.37.003849

[69] Zhu X, Zhu G, Wei C, Kotov LV, Wang J, Tong M, Norwood RA, Peyghambarian N. Pulsed fluoride fiber lasers at 3 μm [invited]. Journal of the Optical Society of America B: Optical Physics. 2017;**34**:A15-A28. DOI: 10.1364/JOSAB.34.000A15